PHOTODECOMPOSITION AND REACTIONS OF HYDROXYL AND HYDROGEN DEFECTS IN POTASSIUM CHLORIDE CRYSTALS
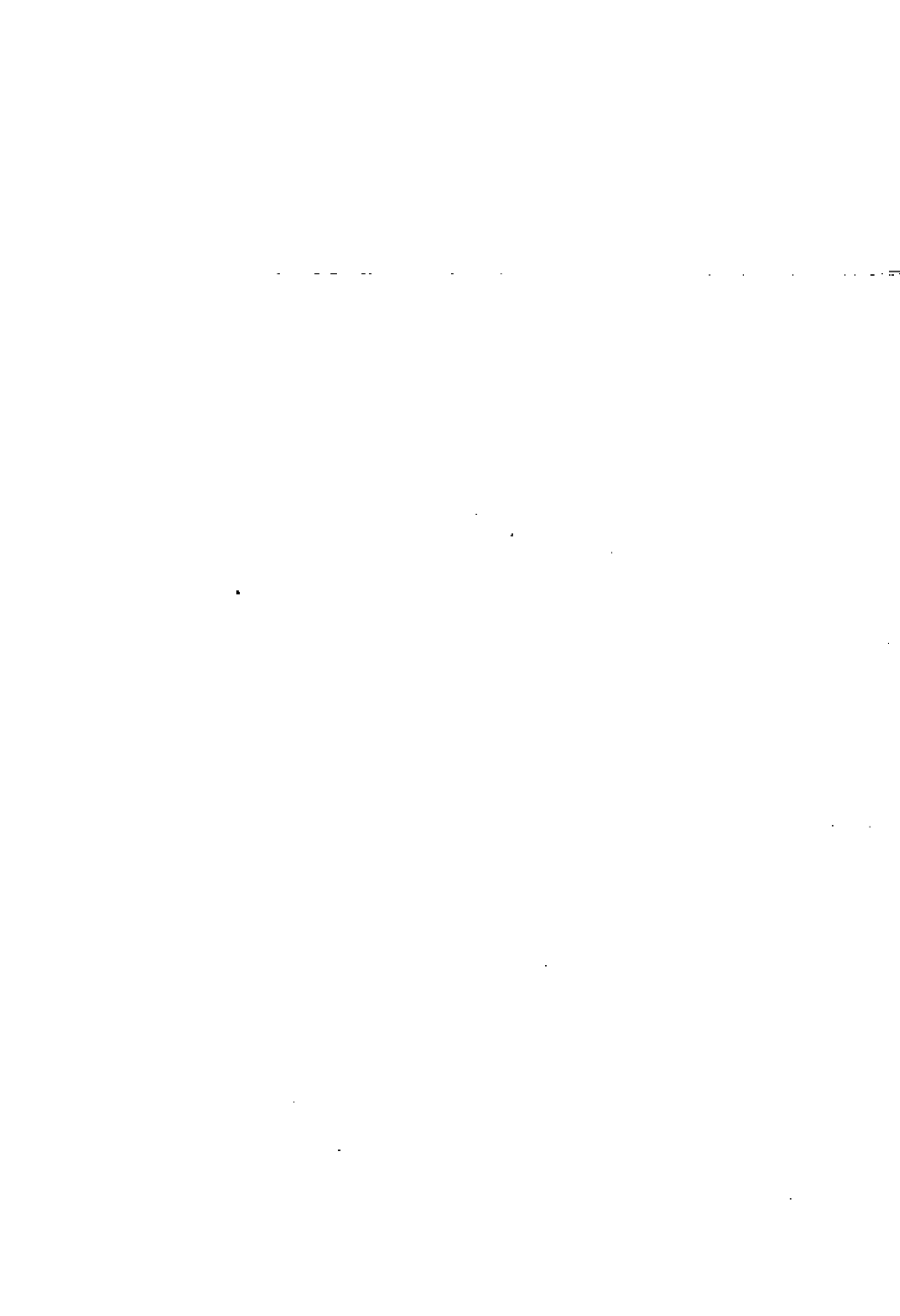
Spero Penha Morato

$\mathcal{CC}\,611$

PHOTODECOMPOSITION AND REACTIONS OF HYDROXYL AND HYDROGEN DEFECTS IN POTASSIUM CHLORIDE CRYSTALS

Spero Penha Morato

Tese para obtenção do Título de "Doutor em Filosofia"
sob a orientação do Prof. Dr. Fritz Lüty.
Apresentada e defendida em 18 de fevereiro de 1975,
no Departamento de Física da Universidade de Utah.

NOTA: Este trabalho foi conferido pelo autor depois de composto e sua redação está conforme o original, sem qualquer correção ou mudança.

UNIVERSITY OF UTAH GRADUATE SCHOOL

SUPERVISORY COMMITTEE APPROVAL

of a dissertation submitted by

Spero Peuha Morato

I have read this dissertation and have found it to be of satisfactory quality for a doctoral degree.

February 18, 1975
Date

Fritz Lüty
Chairman, Supervisory Committee

I have read this dissertation and have found it to be of satisfactory quality for a doctoral degree.

February 18, 1975
Date

Owen W. Johnson
Member, Supervisory Committee

I have read this dissertation and have found it to be of satisfactory quality for a doctoral degree.

February 18, 1975
Date

F. Rosenberger
Member, Supervisory Committee

I have read this dissertation and have found it to be of satisfactory quality for a doctoral degree.

February 18, 1975
Date

William D. Ohlsen
Member, Supervisory Committee

I have read this dissertation and have found it to be of satisfactory quality for a doctoral degree.

February 18, 1975
Date

H. J. Monkhorst
Member, Supervisory Committee
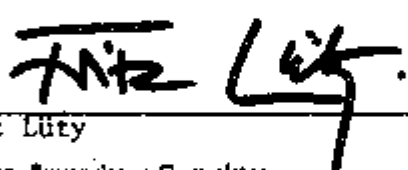
UNIVERSITY OF UTAH GRADUATE SCHOOL

FINAL READING APPROVAL

To the Graduate Council of the University of Utah:

I have read the dissertation of ___Spero Penha Morato___ in its final form and have found that (1) its format, citations, and bibliographic style are consistent and acceptable; (2) its illustrative materials including figures, tables, and charts are in place; and (3) the final manuscript is satisfactory to the Supervisory Committee and is ready for submission to the Graduate School.

___February 18, 1975___
Date

___Fritz Lüty___
Member, Supervisory Committee

Approved for the Major Department

Peter Gibbs
Chairman/Dean

Approved for the Graduate Council

Sterling M. Mc. Murrin
Dean of the Graduate School

TABLE OF CONTENTS

PHOTODECOMPOSITION AND REACTIONS OF HYDROXYL IONS AND HYDROGEN DEFECTS IN POTASSIUM CHLORIDE CRYSTALS

Spero Penha Morato

ABSTRACT

Substitutional OH^- defects in alkali halide crystals can be dissociated by irradiation with UV light into oxygen — and various forms of hydrogen — defects. This photodissociation process was studied over a wide range of temperature (4-300K), and the various hydrogen reaction products were identified by their characteristic electronic absorption (in the UV) and local mode absorption (in the IR range). Besides the well known substitutional and interstitial H^0 and H^- defects, a new hydrogen center was found as the main final reaction product of the photo-dissociation. It is characterized by a single strong IR band at $\omega = 1112$ cm^{-1}, which displays an isotope shift $\omega(H) : \omega(D) = \sqrt{2}$, indicating a localized mode of a charged hydrogen atom in a site of high symmetry. The kinetics of formation and conversion of this defect under UV and X-ray irradiation was studied in detail under a variety of conditions. These experiments allow us to formulate as a structural model a hydrogen ion (H^-) in a body-centered interstitial position with a trapped hole symmetrically shared by the four nearest lattice anion neighbors.

If F centers are additionally present in the crystal, the hydrogen products of the OH^- photodissociation can react with these F centers in various ways. Therefore the UV light induced processes lead to an effective bleaching of the visible F center absorption (color). The possible potential of this process for optical information storage was tested and demonstrated by the UV light production of high contrast, high resolution and thermally stable visible images in the crystals.

I — INTRODUCTION

The objective of this work is a comprehensive investigation of the photodissociation of substitutional OH^- defects in KCl over a wide range of temperatures, including the study of the primary and secondary reaction products of this photodissociation and their interaction or reaction with F centers. The used KCl host material stands as a representative for the large family of cubic alkali halide crystals, while the OH^- ion represents other diatomic molecules of the type XH^- (like SH^-), with supposedly similar properties. The observed phenomena and processes in KCl:OH^- may therefore be regarded as a model case for a large group of (crystal + defect)-systems.

The essential motivation for this investigation can be briefly summarized in terms of several interesting physical aspects of the studied systems and processes:

1 — Substitutional OH^- defects are a prominent impurity in basically all melt-grown and natural alkali halide crystals. Their presence — even in small quantities ($\sim 10^{-5}$) — has pronounced effects on many physical properties of the host crystal, like optical[1,2] dielectric[3,4] and elastic[5,6] behavior, ionic[7] and thermal conductivity,[8] photochemistry[9,10], and radiation damage[11]. Besides this, the presence of OH^- impurities can even influence the photochemical behavior of other lattice defects (like F-centers), as we will show in this work.

2 — Besides being often an unwanted impurity, the OH^- ion — the most simple heteronuclear diatomic lattice defect — is a very interesting entity which has been extensively studied for its own sake. As the OH^- molecule carries an electric dipole moment[12] as well as an elastic dipole moment[13] (due to its nonspherical shape), it gives rise under electric field or stress application to paraelectric and paraelastic ordering phenomena[14,15]. These and many other interesting features have been studied extensively for

the defect in its electronic ground state. Its properties and behavior in the excited state after photo-excitation (like the dissociation treated here) are so far very little understood.

3 — The photo-dissociation of OH⁻ ions makes this defect a direct source of hidrogen atoms or ions, which can occupy various substitutional or interstitial sites in the crystal. Hydrogen defects are the most simple and fundamental chemical impurities in crystals, which — due to their simple structure — are best accessible to a full quantum-mechanical treatment of their properties and interaction with the surrounding lattice. Studies of hydrogen impurities extend beyond alkali halides to many other solid state systems, and are particularly important in metals. Alkali halide crystals are especially attractive and informative for these studies, because the (substitutional or interstitial) hydrogen can be identified not only by UV transitions due to electronic excitation[16], but also by infrared transitions due to the excitation of the (small mass) local modes of charged hydrogen impurities[17,18].

4 — As in many other solid state systems, the process of radiation damage — i.e., the formation of lattice defects by high energy radiation — has been studied extensively in alkali halides[19]. Most important in these studies is the understanding of the elementary formation process, the primary creation of vacancy-interstitial pairs and their secondary reactions at low temperatures. Hydrogen interstitials, created by "optical radiation damage" through photo-dissociation of substitutional OH⁻ or H⁻ impurities, have played and still play a model role in the attempt to understand both the primary process and the secondary reactions of the formed interstitials[18,20].

5 — Alkali halides with color centers and impurities, which give rise to photochemical reactions, have become recently important for possible applications as photochromic media for optical information storage[21] (particularly for the storage of "Bragg-angle holograms"[22]). The photochemical reactions involving OH⁻ and F center defects, treated in this work, allow us to make an (invisible) UV light bleaching process appear as a high contrast bleaching process in the visible range. This feature may make this process attractive for information storage or display involving UV light.

In the following chapter (II), we will give a more detailed account of the physical background which is necessary for the understanding of the performed experiments and their discussion. This will include a survey on the defect structures to be discussed, a summary of the main physical properties of OH defects as well as of H⁻ defects and their reaction products, and a brief digest of the main aspects of the elementary process of defect formation by radiation damage in alkali halide crystals. Chapter III contains a description of the apparatus, crystal preparation and experimental techniques used. In Chapter IV we present the experimental material and discussion about the primary photodissociation of KCl:OH⁻ and KCl:OH⁻+ F systems below 100K. In this same chapter we extend our studies to the photodecomposition of one of the OH⁻ primary products and discover a new and very interesting hydrogen center. In Chapter V and Chapter VI we treat the OH⁻ photodecomposition in the same systems for the 100-200K and 200-300K temperature intervals respectively. Finally, in Chapter VII, we discuss the practical aspects of our systems for U_A center formation and optical information storage.

II — PHYSICS BACKGROUND

A. NOTATION OF THE DEFECTS TREATED IN THIS WORK.

A large number of intrinsic and extrinsic point defects, of both substitutional and interstitial type, will appear in the measurements and discussions of this work. Most of them are well known species, which have been extensively studied in previous work and have been clearly identified in terms of their microscopic defect structures. In spite of this characterization by well established microscopic models, the description of these defects has followed so far mostly a historical and completely illogical and confusing notation system, which is understandable only to the insider. We therefore give, in Table I, a compilation of the point defects treated in this work, listing their structural model, their historical name, and the descriptive symbols. Similarly, we illustrate in Figure 1 these point defects by a schematic representation of their microscopic structure in a <100> crystal plane.

Table I

Survey of the treated point defects in KCl, in terms of their
structural model, their historic notation, and the
symbol which will be used in this work.

| Structural Model	Historic Notation	Symbol
Anion vacancy	α Center	$[\ ^-]$
Electron trapped at anion vacancy	F Center	$[e^-]$
Substitutional hydroxide ion	OH⁻ Center	$[OH^-]$
Substitutional hydrogen ion	U Center	$[H^-]$
Water molecule trapped in an F center	H_2O^- Center	$[H_2O^-]$
	("wet F center")	
Substitutional hydrogen atom	U_3 Center	H^o
Interstitial hydrogen ion	U_1 Center	H_i^-
Interstitial hydrogen atom	U_2 Center	H_i^o
Interstitial chlorine ion	1 Center	Cl_i^-
Interstitial chlorine atom (in < 110>	H Center	Cl_i^o
"crowdion" configuration)		
Interstitial chlorine molecule	H' Center	$(Cl_2^o)_i$
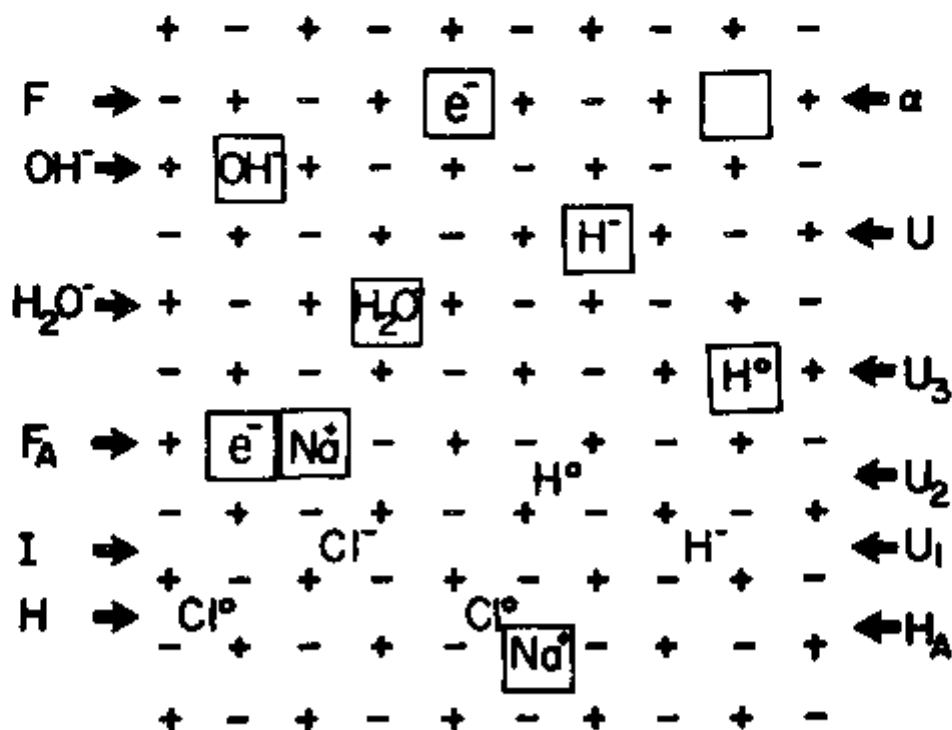
Figure 1 — Structural models of the defect centers treated in this work.

4

In the reaction equations, when we talk about particular defect centers, we will use as much as possible the physical symbols listed in the third column of Table I. (The square box stands for a substitutional, the index "i" for an interstitial site). For the optical absorption bands in the UV visible range, we will, however, use the long established historic notations, i.e., U, U_1 and U_2 band.

B. THE MAIN PROPERTIES OF OH⁻ DEFECTS.

Early observations of alkali halides containing OH⁻ defects showed that when subject to UV or X irradiation the OH⁻ defect could be converted into other defects such as the U and the F centers[9]. From the fact that these reaction products are defects of an anion lattice site, it was concluded that the OH⁻ defect occupies a substitutional place in the lattice. More recently, combined measurements of the macroscopic density and microscopic lattice parameter for the KCl:OH⁻ system confirmed the substitutional model for the OH⁻ defect beyond any doubt[23].

OH⁻ impurities incorporated substitutionally in alkali halides give rise to three types of optical excitation: an electronic, vibrational and librational absorption. The electronic absoption consists of a broad, structureless and asymmetric band the UV which shows only a small narrowing effect when the crystal is cooled to low temperatures. It was found[2,14] that the position of the UV absorption maximum of the OH⁻ defect in thirteen alkali halides follows an empirical relation (first observed by Ivey for F centers) which connects the nearest neighbor separation (d) with the maximum of the band (ν_{max}) in the form of

$$\nu_{max} = 691 . d^{0.95}$$

This empirical relation supports the analogy of the OH⁻ UV absorption with the first excitonic absorption of the host crystal. To explain the excitonic spectra os alkali halides, Hilsch and Pohl[24] suggested that the absorption of a photon would induce an electron charge transfer from a halogen ion to a nearest neighbor alkali ion. This process could successfully predict the positions of the excitonic bands not only for the pure crystals but for halogen impurity ions as well[25]. The similarity of the fluoride ion F⁻ with the OH⁻ ion suggests somehow that one can qualitatively explain the properties of the OH⁻ transitions with the same type of charge transfer model. Theoretical calculations on the electronic absorption of the OH⁻ center by Chae and Dick[26] followed essentially this model, treating the ground state as that the free OH⁻ ion and the excited state as a charge transfer state

The IR spectrum of OH⁻ ions in alkali halides shows a vibrational absorption in the near IR produced by the optical excitation of a stretching vibrational mode of the OH⁻ molecule and a librational mode[27] in the far IR due to the excitation of the angular motion of the OH⁻ ion. Either the UV or the IR absorption provides a good method for the optical determination of the OH⁻ concentration. From concentration measurements by titration of KOH doped crystals[7,14], one can determine the oscillator strength for the UV and IR bands, thus establishing a calibration of concentration vs. absorption constant.

Extensive measurements have been done in the last decade on the electric field- and stress-ordering (paraelectric and paraelastic alignment) of OH⁻ defects in various alkali halides. These measurements have established the magnitude and symmetry of the electric and elastic dipole moments, and have determined the polarization characteristic of the UV transition of the defect. In most alkali halide host crystals (among them KCl), the OH⁻ defect is found to be oriented by the crystal field in a <100> direction. The UV transition of the OH⁻ defect is mainly polarized perpendicular to the dipole axis, with a small admixture of oscillator strength f in the dipole direction[12] ($f_\parallel/f_\perp \approx 0.3$).

Two types of phenomena are so far available which give some information about the electronic excited state of the OH⁻ defect:

a) A Stokes shifted emission of fluorescence (in the near UV range), which appears at low temperature as a consequence of optical excitation in the UV OH⁻ absorption band[28,29].

b) Photodissociation of the OH⁻ molecule as a consequence of the UV excitation[20].

The photodissociation process of OH⁻ defects, which has been studied in some aspects previously by several authors, is the subject of this work and will be treated in Chapters IV, V and VI.

The emission spectra of the OH⁻ center display a well resolved and equally spaced structure (the separation of which corresponds to the vibrational frequency of the OH⁻ molecule) with peak intensity decreasing monotonically to lower energies. From these and other properties, it was concluded that the emission bands are due to radiative transitions to different vibrational levels of the ground state and that the highest energy band arises from a transition between the lowest vibrational levels of the two electronic states. The fact that the emission bands showed temperature broadening reflects the strong coupling of the electronic states to lattice vibrations, as it is typical for color centers.

C. THE ELEMENTARY LOW TEMPERATURE RADIATION DAMAGE IN PURE KCl.

Radiation damage processes in alkali halides have, for a long time, stirred the curiosity of many researchers. Extended work in this field has brought up a large amount of background information on the detection, identification and properties of the defects produced by radiation. However, in spite of a long and intense exploration in this complex field, it was only very recently that the most simple and fundamental questions have received more concentrated attention and first reliable answers.

Starting with the most basic question for the understanding of radiation damage in alkali halides we should ask: What is the elementary process of defect formation by ionizing radiation at low temperatures?

Neglecting a long history of various models and mechanisms, the present picture is about like this: Ionizing radiation and light absorbed in the fundamental region of the crystal produces at low temperatures (below 10K) Frenkel defects in the anionic sublattice of the crystal. Two types of anionic defects are formed:[30] charged Frenkel pairs, consisting of an anion vacancy and interstitial anion (α and I center)

$$\boxed{Cl^-} + h\nu \rightarrow \boxed{-} + Cl_i^- \tag{1}$$

and neutral Frenkel pairs, consisting of an anion vacancy with an electron (F-center) and an interstitial chlorine atom (H-center)

$$\boxed{Cl^-} + h\nu \rightarrow \boxed{e^-} + Cl_i^0 \tag{2}$$

Measuring the growth curves (formation rates) under constant irradiation, one observes that considerably more charged Frenkel pairs are formed compared to the neutral ones (in KBr, e.g. the ratio is about 6:1)[31]. Recent short-time measurements with pulsed irradiation techniques[32,33] showed however that the neutral pairs are produced with high efficiency in a very short period (of the order of nanoseconds), while the charged pairs are not yet observed during this initial fast process. This led to the conclusion that neutral Frenkel pairs are the primary products of the radiation damage process. Apparently the charged pairs are subsequently formed due to an electronic process that transfers an electron from an F to an H center. This electronic process is a secondary effect which could, for instance, be produced by the ionizing radiation, or through excitation of an F center electron by intrinsic luminescence radiation.

With the F and H center being generally accepted as the primary products of radiation damage, the next step is to understand how they are formed. The present understanding of the sequence of events which lead to the formation of F and H center pairs can be summarized as follows[34]:

UV or X-rays ionize one lattice halogen ion and lead to the formation of a Cl_2^- molecular ion occupying two adjacent anion sites in the <110> direction (V_k center). This entity ("self-trapped hole or V_k center") is well known and investigated by optical and magnetic techniques. In this V_k center configuration, the two Cl^- ions are closer to each other than in a normal regular lattice. This means that something like two anion vacancies are formed opposite each other in a <110> configuration and with the Cl_2^- molecule ion in between. These two vacancies (each with an effective $+ e^+/2$ charge) are attractive for electrons which can be bound in an excited $2p_z$ state of this double well potential. The excited electron, which occupies the $2p_z$ state of the V_k center when relaxing, forces the Cl_2^- molecule ion to move to one of the normal anion sites while the electron will be entirely localized into the <110> neighboring anion site forming a 1s (singlet-triplet) state with the Cl_2 ion. Due to the higher electronic affinity of this vacancy compared to the semi-vacancies occupied by the $2p_z$ electron, this relaxation $2p_z \rightarrow 1s$ process will give away enough energy to force the Cl_2^- molecule ion to move in a <110> sequence of replacement collisions. The Cl_2 molecule ion will finally be stabilized in a <110> oriented crowdion configuration (H center), well separated from the 1s electron and anion vacancy left behind (F center). It should be mentioned that alternatively to the process, the $2p_z$ electron can make a radiative transition to the 1s state and then, from there, recombine with the V_k center causing the emission of the so-called "intrinsic luminescence". It has been found empirically that in many crystals the quantum efficiency of this luminescence behaves in its temperature dependence supplementary to the efficiency of the above described radiationless defect formation process, as it would be expected in this model.

No detailed explanation or mechanism is available so far to account for the before mentioned fact that, under further irradiation, an electron tranfer from the F to the H center takes place; so, as a net result, more charged Frenkel pairs are formed compared to the primary neutral pairs.

The thermal stability of the two kinds of Frenkel pairs shows a parallel behavior which reflects an apparently very similar physical process behind the thermal destruction or recombination of pairs. In both cases the recombination process occurs via two main distinct temperature steps. For the charged pairs, a first sharp decrease of the interstitial band (at ~ 12K) indicates that the more closely spaced ("spatially correlated") pairs are annihilated. At about 20K, a broader step indicates the annihilation of widely separated ("spatially uncorrelated") pairs[35]. In both steps the thermally mobile interstitial ions recombine with the vacancies reconstructing the perfect lattice.

The neutral interstitial (H center) becomes thermally annealed in two steps at about 10 and 40K[36]. Three possibilities for the annihilation of this interstitial are known:

a) recombination with the F center, restoring the perfect lattice;

b) trapping by small substitutional defects (like Li^+ or Na^+) which can stabilize the interstitial (as a so-called "H_A-center" or historically "V_1-center") to rather high temperatures (e.g. 113K for $KCl:Na^+$)[37];

c) trapping of the mobile interstitial by another H center, froming an interstitial pair ("H center". or historically V_4 center). This pair center again has a high thermal stability[38].

D. THE H^- DEFECT (U CENTER) AND ITS MAIN PROPERTIES AND PHOTO-REACTIONS.

Hydrogen ions (H^-) can be incorporated substitutionally in alkali halides, as was first demonstrated by Pohl[39,40]. These socalled U centers produce a strong structureless electronic absorption band in the UV, the maximum of which occurs for KCl at 214 nm. These centers also produce a narrow

absorption line in the infrared range (at 502 cm^{-1} for KCl), due to a strongly localized vibration of the hydrogen ion, well above the phonon frequencies of the lattice[17].

At low temperatures (T < 80K), irradiation with UV light in the U band leads to the expulsion of the H$^-$ ion from its lattice site to an interstitial position (U$_1$ center) with an empty anion vacancy (α center) formed at the original H$^-$ site. This process can be represented by the following reaction.

$$\boxed{H^-} + h\nu \rightarrow \boxed{-} + H_i^- \tag{3}$$

It is evident that this process, produced at low temperatures by the absorption of a UV light quantum, is a low energy analog to the formation of the intrinsic charged Frenkel pair produced by high energy radiation in the pure crystal (Equation 1). In the case of the H$^-$ defect, an "extrinsic charged Frenkel pair", consisting of anion vacancy and H$^-$ interstitial (instead of Cl$^-$ insterstitial) is formed. The H$^-$ interstitial defect (U$_1$ center) gives rise to a very broad structureless electronic absorption in the UV range and a local mode absorption in the IR region (around 12 μ in KCl). The latter displays, at lowest temperatures, a fine structure consisting of several groups of sharp lines that correspond to H$^-$ interstitials with various spacial correlations and interactions to the anion vacancy ("correlated extrinsic Frenkel pairs")[18].

Subsequent prolonged broad band irradiation in the UV will excite the U$_1$ absorption of the H$_i^-$ ion, leading to its ionization and transfer of the electron into the anion vacancy:

$$\boxed{-} + H_i^- + h\nu \rightarrow \boxed{e^-} + H_i^o \tag{4}$$
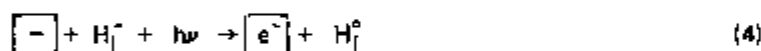
Thus by this secondary process, the extrinsic charged Frenkel pair is converted into a neutral pair, consisting of an F center and hydrogen atom interstitial (U$_2$ center). The latter defect is characterized by an electronic absorption band in the UV (at 236 nm in KCl), and has been extensively studied by EPR and ENDOR techniques[41,42].

A fourth possible form of hydrogen center in an alkali halide lattice is the hydrogen atom occupying one anion site (U$_3$ center)[43]. However, due to a possible small oscillator strength or to very low concentrations experimentally obtained so far, it was not possible to optically identify this center. Nevertheless, EPR and ENDOR measurements did reveal the existence and microscopic structure of the U$_3$ center.

The thermal stability of the negative interstitial hydrogen shows the same general behavior as discussed for the intrinsic chlorine interstitials: Thermal annealing curves with characteristic temperature steps are observed. The vacancy-H$^-$ interstitial pair shows a first sharp annealing step at about 90K and a broader one around 180K[18]. Measurements of this annealing in the H$_i^-$ local mode absorption show directly the annealing at low temperatures of certain groups of local mode lines which correspond to spacially correlated Frenkel pairs (the H$_i^-$ local modes are split by the interaction with the vacancy); at higher temperatures (~ 180K), the (unsplit) local mode absorption line of the free uncorrelated H$^-$ interstitial is annealed.

In the thermal annealing of the neutral hydrogen interstitial (U$_2$ center) only one step (at ≈ 108K) is observed, showing that apparently there is only very little interaction with its anti-center the F center. The interstitial hydrogen atom, becoming thermally mobile, should in principle be able to anneal the F center and restore the original U center. This, however, is not observed at all experimentally[44]. From the thermal disappearance of the atomic hydrogen center it must be concluded that it recombines with other hydrogen atoms to form stable interstitial hydrogen molecules[45].

Several "perturbed hydrogen centers" with the hydrogen located close to other impurities have

been studied recently. Spacially correlated U·H center pairs were found to display a broadening and shifting of the U center UV absorption and a removal of the degeneracy of its IR local mode absorption[20,46]. Pairs of mutually perturbed U centers (H⁻H⁻pairs) were also the subject of recent investigations[47]. These <110> oriented H⁻H⁻pairs produce several lines in the IR local mode region that could be interpreted with coupled oscillator models.

The presence of additive impurities can produce other forms of perturbed hydrogen centers. For example, a metallic impurity like Na^+ in KCl situated in one of the six nearest neighbor sites of an H^- center (then a U_A center) will cause the splitting of the triply degenerate local mode vibration of the H^- center. This splitting is due to the reduction of the O_h symmetry of the perfect lattice into C_{4v} symmetry.

III – EXPERIMENTAL PROCEDURES, APPARATUS AND SAMPLE PREPARATION

A. CRYOSTAT AND SAMPLE HOLDER.

Most of the optical measurements, optical and thermal treatments were carried out with and He^4 optical cryostat made by F. X. Stöhr (Germany). This cryostat was provided with four windows which permitted parallel and crossed optical beam experiments, together with the possibility of exchanging windows according to the specific spectral requirements of the experiment. A variable temperature tail for this cryostat was designed and built, based on the principle of exchange gas as a thermal switch[48] (Figure 2). This tail consisted of a stainless steel tube of two-inch outer diameter and about 14-inch length. Between the LHe^4 bath tank and sample holder a 2-inch long exchange gas chamber was soldered, made
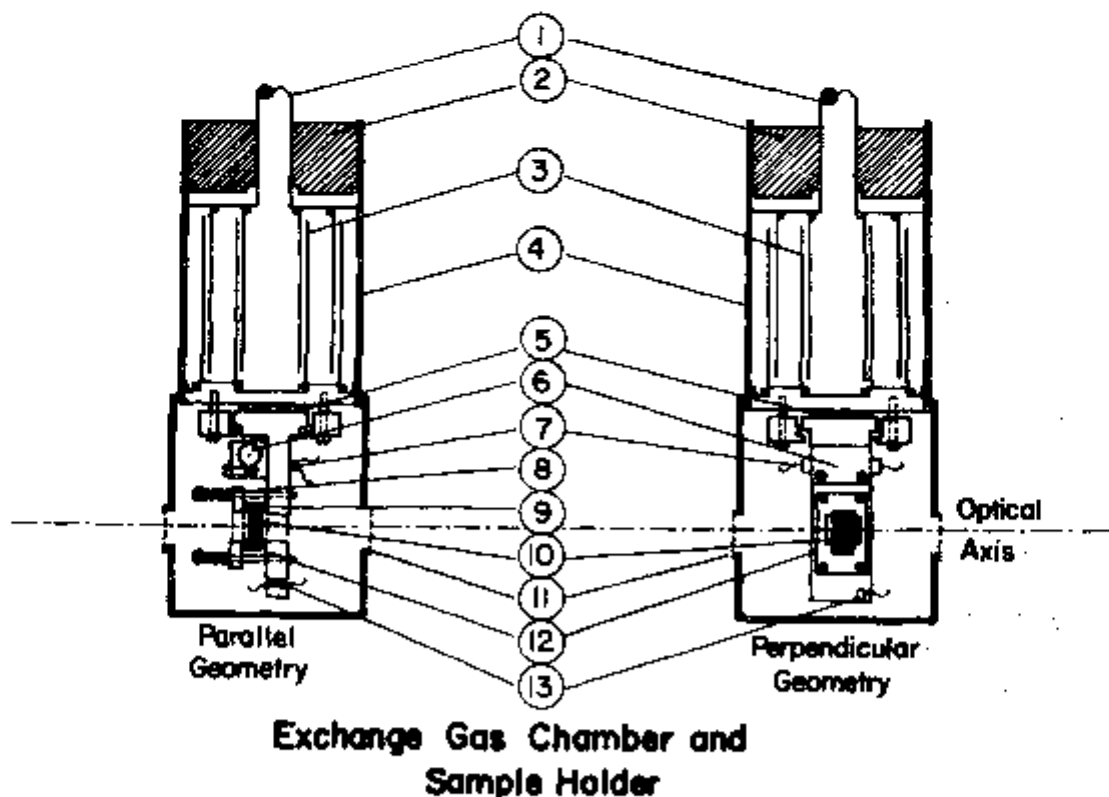

Exchange Gas Chamber and
Sample Holder

Figure 2 — Exchange gas camber and sample holder. (1) He exchange gas inlet; (2) LHe bath; (3) Concentric Cu tubing; (4) Exchange gas chamber; (5) In foils; (6) Heater block; (7) Cu const. thermocouple; (8) Cu mask; (9) In pads; (10) Sample; (11) Windows; (12) Cu block; (13) Thermistor.

out of the same stainless steel tube with 1/4-inch thick copper caps. This chamber contained four concentric copper tubes with one end alternatively welded to the bottom and top copper caps. In this way they were placed with out mechanical contact at a very close distance from each other, thus facilitating the thermal contact when the operation with exchange gas was necessary. Weep holes were provided in these internal tubes to increase the gas circulation inside the chamber. A vacuum of about 10^{-5} Torr was established in this chamber when no thermal contact was required between the sample holder and LHe bath. This was the case when a sample temperature was established with heater higher than the (LHeT or LNT) bath temperature.

The sample holder was designed to meet the most variable requirements such as crossed or parallel optical beam geometries. It consisted of an L-shaped piece of copper machined out of a solid block. It was pressed against the bottom plate of the exchange gas chamber by a circular brass flange, with indium foils interposed between the mechanical parts to increase the thermal contact (Figure 2). In this way, quick changes of geometry were possible just by releasing the flange screws and rotating the sample holder. Soldered to the sample holder was a heater element which consisted of a copper block with a 900Ω 10 W carbon resistor wrapped by copper foils and tightly fitted to the copper block. The high power dissipation characteristics of this heater were necessary in order to achieve quick temperature changes, different heating rates and high temperature annealings. The heater element was powered by a Variac transformer.

B. ADDITIVE COLORATION AND HYDROGENATION OF CRYSTALS.

Additive coloration is the introduction of a nonstoichiometric excess of alkali metal into the alkali halide crystal. This process is achieved by heating the crystal close to its melting point under an alkali metal vapor atmosphere. Neutral vaporized metal atoms react with surface halogen ions and loose their electron which is transferred to the conduction band. The halogen ion will leave a vacancy behind and form with the alkali ion another layer of the crystal. The halogen vacancy will thermally diffuse through the crystal and eventually trap an electron to form an F center, giving the crystal the F center color. A relative fast quench to room temperature will freeze in the high temperature F center equilibrium. This mechanism, as proposed by Mott and Gurney[49], does not require the diffusion of the metal ion through the crystals contrary to what was thought previously[50]. Each absorbed alkali ion will create a correspondent anion vacancy as in a Schottky defect formation process. Several experiments, like the additive coloration of KCl either in K or Na vapor[51], confirmed this picture.

To additively color our samples we employed the method described by Van Dorn[52] with some modifications. In this method the F center concentration was obtained by a controlled vapor pressure of the metal vapor using an excess pressure of nitrogen gas. We used a low fixed pressure of nitrogen gas and varied the liquid potassium temperature, thus varying its vapor pressure. Using an intermediate calibration curve from Van Dorn and Rögener's methods[53], which give the F center concentration as a function of the potassium vapor pressure, we were able to obtain quite reproducibly F center concentrations on the order of 10^{16} to 10^{18} cm^{-3}.

Hydrogenation of additively colored sample consists in the controlled diffusion of hydrogen into the crystal under high temperature and hydrogen pressure. By heating the crystal at $650°C$ under 20 atmospheres of hydrogen gas, hydrogen molecules diffuse into the crystal and react with the F centers, producing substitutional hydrogen ions (U centers):

$$H_2 \;+\; 2\boxed{e^-} \rightarrow 2\boxed{H^-} \tag{5}$$
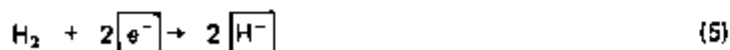
C. SAMPLE PREPARATION.

The KCl crystals were grown from the melt by the Kyropoulus method under a controlled argon gas atmosphere[54], in the Utah crystal growth laboratory. The starting crystal material was ultrapure grade from E. Merck AG Darmstadt (Germany). Some ultrapure material was subjected to a pretreatment

with HCl at high temperatures to eliminate as much as possible traces of OH⁻ or oxygen impurities. In other crystals, KOH was intentionally added to the melt in controlled amounts in the range of 10^{-3} to 10^{-4} mole percent to dope the crystal with the desired OH⁻ content.

The samples were cleaved from the middle of the additively colored or hydrogenated crystals to avoid the (possibly contaminated) surface sections. Sample dimensions ranged from .30 to 10.0 mm thickness for the optical path according to the experimental requirements. The samples were mounted on the sample holder by compression with a spring-loaded copper frame. Indium foils were always used to provide a better thermal contact between sample and holder and also as an optical mask to avoid the bypass of the light beam. Additively colored samples were handled under safe red light from the time of their quenching to the mounting in the sample holder. This was done in order to avoid any spurious photochemical process. The crystals were heated for thirty seconds at about 400°C and quenched on a copper block under a dry nitrogen atmosphere, then immediately transferred in the dark to the sample holder. With this procedure, a very pure and uniform distribution of F centers was obtained.

D. TEMPERATURE CONTROL AND THERMOMETRY

Between LNT and RT temperature was automatically controlled by a Leeds Northrup Millitemp controller, the sensor of which was a copper constantan thermocouple, also from Leeds Northrup, soldered to the heating element. With liquid nitrogen in the LHe tank and a low pressure of exchange gas ($< 50\mu$), any temperature between LNT and RT could be obtained with a precision of $\pm \sim 1K$. In this range the temperature was either monitored and recorded with the copper constantan thermocouple or measured with a NTC carbon resistor from Keystone Carbon Co. Resistance measurements were made with a Leeds Northrup Wheatstone Bridge Model #4760.

Below LNT temperature measurements were carried out with o.1W, 100Ω Allen Bradley carbon resistors[55] placed in the sample holder block (glued to the sample holder with GE varnish #7031 or Dow Corning silicone grease). The thermal contact between the thermistor and sample was improved by grinding it slightly flat with fine emery paper, increasing in this way its contact area.

The resistance values against temperature were calibrated for different known temperature points like LHeT, LNT and dry ice temperature and the extrapolation from measured temperatures was made by means of the empirical relation

$$\left(\frac{\log R}{T}\right)^{\frac{1}{2}} = A \log R + B \tag{8}$$

where A and B are constants characteristic of the individual thermistor. A PDP-11 computer was programmed in BASIC to produce an interpolated table of temperature values versus resistance. Deviations smaller than 1% were detected from recalibrations of these thermistors. Below LNT the temperature control was achieved manually. All the leads going to the sample holder were anchored to the LHe bath with thermal compound (Wakefield Engineering Co.) before they would reach the sample holder to avoid heat flow from the outside.

E. IRRADIATION PROCEDURES.

For undispersed UV + visible light irradiations, we used a 150W Xenon lamp from Hanovia #901C-11, mounted in a Bausch Lomb lamp housing and equipped with UV grade quartz condenser lens system. In some cases, when more intense light in the F center region was required, we used a 200W Mercury HBO lamp from Osram. For monochromatic irradiations in the UV region we used the Xenon lamp mounting attached to a Bausch and Lomb grating monochromator #33-86-01 with 2700 grooves

per mm. The band pass used was approximately 20 nm. In general, higher order spectra were not eliminated. When it was necessary to obtain a fairly pure monochromatic irradiation, two monochromators were coupled in a tandem arrangement

F. OPTICAL ABSORPTION MEASUREMENTS.

The variety of experimental methods required a great versatility in the optical measurement. Therefore the cryostat was mounted in a movable frame together with the high vacuum system, temperature controller, recorder and optical bench. This frame could be easily moved from one spectrophotometer to another or to fixed optical benches, according to the experimental requirements. The cryostat had its optical height standardized to match the optical beam height of the spectrophotometers. A set of interchangeable windows provided adequate transparency in all optical ranges of interest.

Optical absorption measurements were carried out with the Cary 14 or Beckman IR-12 recording double-beam spectrophotometers. The Cary 14 covered a range from 190 nm to $2.5\,\mu$. Infrared data beyond $2.5\,\mu$ were taken with the Beckman IR-12 which covered the range from $2.5\,\mu$ to $50\,\mu$. Special care had to be taken in the far infrared region (hydrogen local mode spectroscopy). In order to obtain a good signal-to-noise ratio, the noise level was reduced by constantly purging the instrument plus cryostat set-up with dry nitrogen gas avoiding the atmospheric absorption from water vapor. The resolution obtained with the Cary 14 was around 1 nm. The resolution obtained with the Beckman IR-12 was variable, from 1 to $12\,cm^{-1}$ according to the experimental requirements.

The determination of concentration for the centers involved in this work was done by using the well known Smakula formula:

$$N \cdot f = const\ \frac{n}{(n^2 + 2)^2}\ K_{max}\ H \tag{7}$$

where

N = concentration in cm^{-3}
f = oscillator strenght
n = refractive index of the crystal at the band's maximum
K = absorption constant
H = width at half maximum

The spectrophotometer measured optical densities which relate to the absorption constant in the following way: the decrease in intensity as the light crosses the sample is given by:

$$I = I_o\ e^{-Kd} \tag{8}$$

where d is the thickness of the crystal.

Optical density is defined as

$$O.D. = log\ \left(\frac{I_o}{I}\right) \tag{9}$$

so the absorption constant is given by

$$K = \frac{2.303\ O.D}{d} \tag{10}$$

Substituting the proper values into Smakula's equation, we obtain simplified forms for the calculation of the concentration of F and U centers at room temperature[4,5]:

$$N_F = 1.09 \times 10^{16} \times \left(\frac{O.D.}{d(cm)}\right) \qquad \text{for F centers} \qquad (11)$$

$$N_U = 1.27 \times 10^{16} \times \left(\frac{O.D.}{d(cm)}\right) \qquad \text{for U centers} \qquad (12)$$

For calculation of the OH⁻ concentration we used the calibration described by B. Fritz, et al[7]. The concentration determination of other centers studied in this work followed the same procedure with the Smakula's formula described above

IV – PHOTOREACTIONS BETWEEN 0 AND 100K.

RESULTS AND DISCUSSION

A. INTRODUCTION.

As already mentioned in Chapter II, the excitation of the OH⁻ electronic transition can produce the photodissociation of the OH⁻ ion. The primary products of this process, as first proposed by Kerkoff[9], consist of an interstitial hydrogen atom (H_i^o center) and an oxygen ion left at the original OH⁻ lattice site. This photodissociation process can be represented by the following equation:

$$\boxed{OH^-} + h\nu \ \rightarrow \ H_i^o + \boxed{O^-} \qquad (13)$$

In our effort to study comprehensively the photodissociation of the OH⁻ defect in KCl, we covered the whole temperature range from liquid helium to room temperature. In order to give a reasonable structure in the presentation and discussion of the extended material we divided the temperature range into three intervals. The choice of these intervals was suggested by the thermal stability of the main reaction products of the OH⁻ photodissociation. The first and most important temperature interval was chosen to be the one in which the H_i^o center is thermally stable, that is, below about 100K. Below 200K we find other centers like H_i^- or H_2O thermally stable and this defined the upper limit of our second temperature interval. Above 200K, the range around room temperature, apparently none of the products of the OH⁻ photodissociation is stable any more. This range is of particular interest for applications of photochromic effects.

The introduction of F centers into the KCl:OH⁻ crystals was done with the intention to extend this study into the dynamics of the OH⁻ photodissociation products and subproducts. F centers are the simplest defects that can be extrinsically added in large quantities (up to 10^{19} cm⁻³) in alkali halides by a nonstoichiometric excess of alkali metals, as explained in Chapter III. It is an excellent probe to test the behavior of other centers like H_i^o through their interactions and recombinations. Our experimental procedures therefore consisted, in each temperature range, of a study of the OH⁻ photodissociation in pure KCl:OH⁻ crystals, followed by a subsequent study where we repeated the same procedures with KCl:OH⁻ crystals containing F centers. In this way it was possible to make a direct comparison between the two systems and analyze the role played by the F centers. In a later stage we proceeded with the study of the photochemistry of the OH⁻ secondary products.

B. PRIMARY PRODUCTS OF THE OH⁻ PHOTO-DISSOCIATION AND THEIR INTERACTION WITH F CENTERS.

The electronic absorption band of the OH⁻ defect in KCl appear at 204 nm rather close to the

low energy tail of the fundamental electronic absorption of the crystal. For KCl, like most of the alkali halides, the OH⁻ absorption is broad (halfwidth about 0.5 eV), structureless and asymmetric, and has an oscillator strength of about 0.13[7,23]. (See Table 2).

<div align="center">Table II</div>

<div align="center">Peak positions, halfwidths and oscillator strengths of the
UV or IR absorption of various defects in KCl.</div>

Center	L HeT			LNT		
	Band Max	Half-width	Oscillator Strength	Band Max	Half-width	Oscillator Strength
$\boxed{OH^-}$	6.05 eV	0.60 eV	0.12	6.07 eV	0.61 eV	0.13[a]
H_i^o	5.27 eV	0.38 eV	0.32	5.27 eV	0.40 eV	0.33
$\boxed{H^-}$	5.84 eV	0.31 eV	0.72			
Cl_i^o	3.69 eV	0.65 eV	0.33			
			0.29[b]			
$\boxed{H_2O^-}$				2.38	0.28	0.05
$\boxed{H^-}$				502 cm⁻¹	8 cm⁻¹	0.50[d]
H_x^-				1112 cm⁻¹	12 cm⁻¹	0.35[e]

a. B. Fritz, F. Lüty and J. Auger, Zeits. Physik 174, 240 (1963).
b. B. J. Faraday and W. D. Compton, Phys. Rev. 138, A893 (1965).
c. In Figure 27, we approximated the H_2O^- spectra into four Gaussian bands and calculated the oscillator strength of the most intense band (maximum at 521 nm)
d. B. Fritz, V. Gross and D. Bäuerle, Phys. Stat. Sol. 11, 231 (1965).
e. To estimate the oscillator strength of the H_x^- center, we assumed in Figure 11 B that the "missing" hydrogens were all converted in H_x^- centers.

We photodissociated the OH⁻ defect in two different temperature ranges (LHeT and LNT) as displayed in Figure 3. By irradiation into the OH⁻ band we obtained its decrease accompanied by the increase of two other bands, due to the H_i^o and the O⁻ centers. Only the long wavelength tail of the O⁻ band could be measured due to the spectral restrictions of the spectrophotometer.

H_i^o centers produced by the photodissociation of OH⁻ centers should be spatially independent of their anti-centers O⁻ . This means that any molecular ion of the form XH⁻ (X is a member of group VI), if it can be photodissociated, will produce unperturbed and isolated H_i^o centers. This was verified by analysis of the U_2 band shape and magnetic resonance spectra of the H_i^o center[9,42,43,57].

Together with Prof. W. D. Ohlsen, we set up an experiment to verify the paramagnetic resonance characteristic of the O⁻ defect. Although we could detect the presence of the H_i^o center by its magnetic resonance after we did the OH⁻ photodissociation, we were unable to observe any resonance of the O⁻ defect. A similar negative result in the attempt to detect the O⁻ defect from reaction of Equation 13 by EPR was obtained by Spaeth[58].

However, O^- defects have been observed by their paramagnetic resonance (and optical absorption) as a result of photochemical processes in other systems ($KCl + O_2^- + UV$ irradiation). It is not understood at all why this same EPR O^- signal does not appear as a consequence of our photodissociation process in Equation 13. As both the OH^- model and the H_i^o model are confirmed beyond any doubt, the third necessary partner in this reaction must be a O^- defect. Even if in this process the O^- would leave the vacancy and go to an interstitial place, it should produce an EPR signal.

We will assume in the following that the third partner in the reaction in Equation 13 is an O^- defect, though we realize the question raised by the missing EPR signal. As all the further treated photoreactions at low temperatures will involve only the hydrogen and not the oxygen, the question about the exact structure of the oxygen defect is not too relevant for our further considerations.
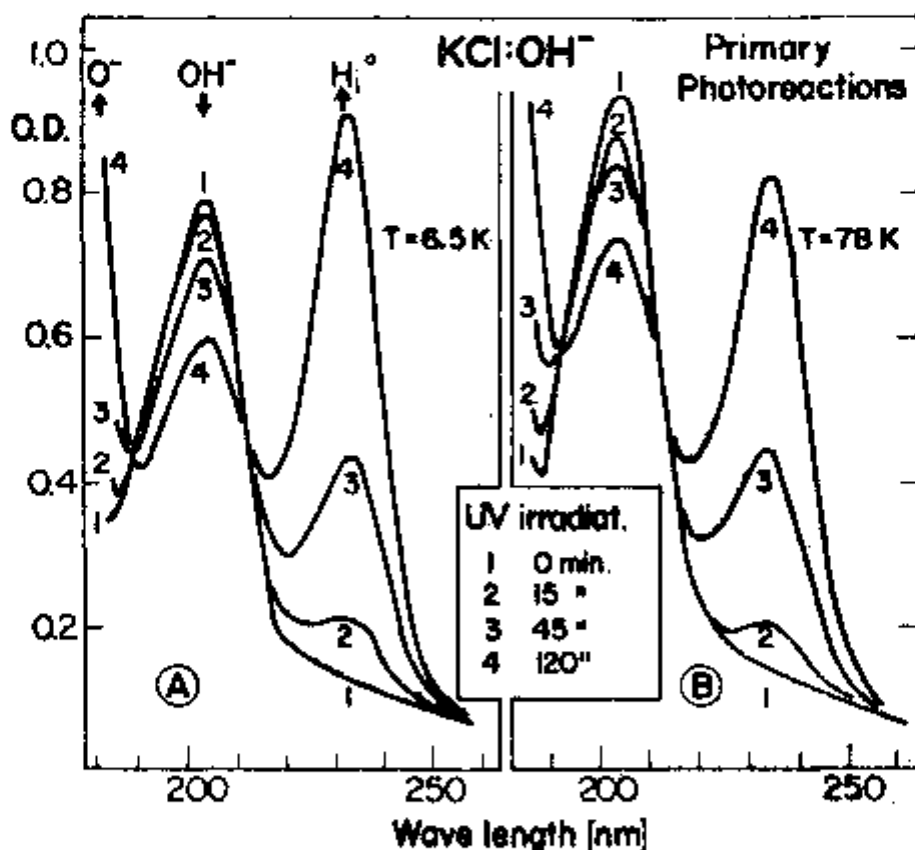

Figure 3 — Optical absorption spectra of a $KCl:OH^-$ crystal showing the primary products of OH^- photodecomposition under OH^- light (204 nm) after different irradiation times at 6.5K (A) and 78K (B).
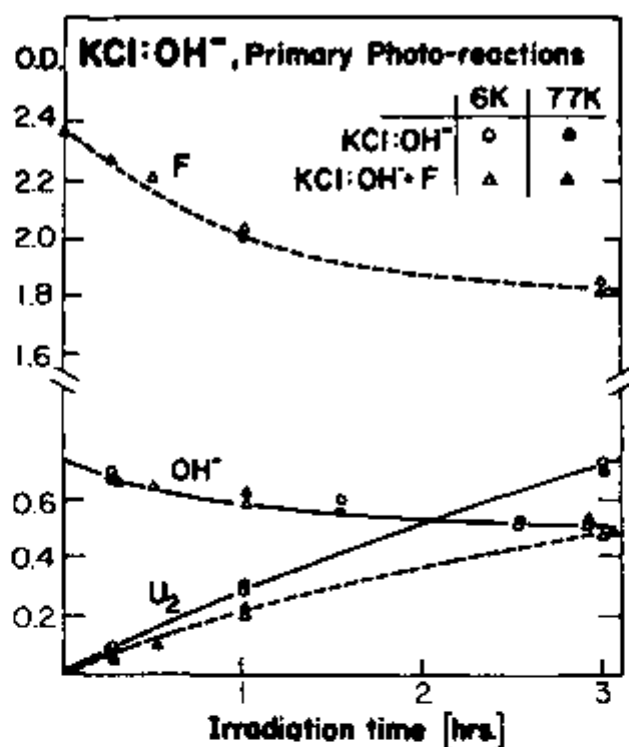
In the presence of F centers, the optical photodecomposition of OH⁻ shows basically the same spectral changes: a decrease of the OH⁻ and an increase of the H_i^o (U_2) band (Figure 4); additionally one observes a decrease of the F band. In Figure 5 we plot these spectral changes versus the irradiation time, and in Figure 6 we compare the OH⁻ decrease with the U_2 band increase, all this for both KCI:OH⁻ and KCI:OH⁻+ F crystals and at 6K and 77K as well. The following results appear:

a) In the pure KCI:OH crystal, the OH⁻ center decay curve and H_i^o center growth curve shown in Figure 5 indicate a process which has a temperature independent quantum efficiency. In Figure 6, we plotted the OH⁻ band decrease vs. the U_2 band increase and obtained a straight line which is a necessary but not sufficient condition for the one-to-one process assumed in Equation 13. As we will see later, the assumption of a one-to-one process will lead to the well known oscillator strength ratio between the two bands.

b) In the KCI:OH⁻ crystal containing F centers, the decay of the OH⁻ band is not affected by the presence of F centers (Figure 5). However, the H_i^o center growth curve indicates a smaller (also temperature independent) quantum efficiency compared to the "pure" KCI:OH⁻ crystal. In Figure 6, we plotted the OH⁻ band decrease vs. the U_2 band increase and again obtained a straight line with a bigger slope compared to the "pure" KCI:OH⁻ crystal. One may conclude from this fact that the same amount of OH⁻ center destroyed in both systems brings, in the presence of F centers, less H_i^o centers than it did in the "pure" KCI:OH⁻ crystal.

Figure 4 — Optical absorption spectra of a KCI:OH⁻ crystal containing F centers, the primary products of OH⁻ photodecomposition in the presence of F centers and the F center reduction after different UV irradiation times at LNT. The dashed line shows further reduction of F and U_2 bands after subsequent F light illumination.

Figure 5 — Buil-up and decay curves for OH⁻, F and U_2 bands involved in the primary OH⁻ photodecomposition process at 6K and 77K.
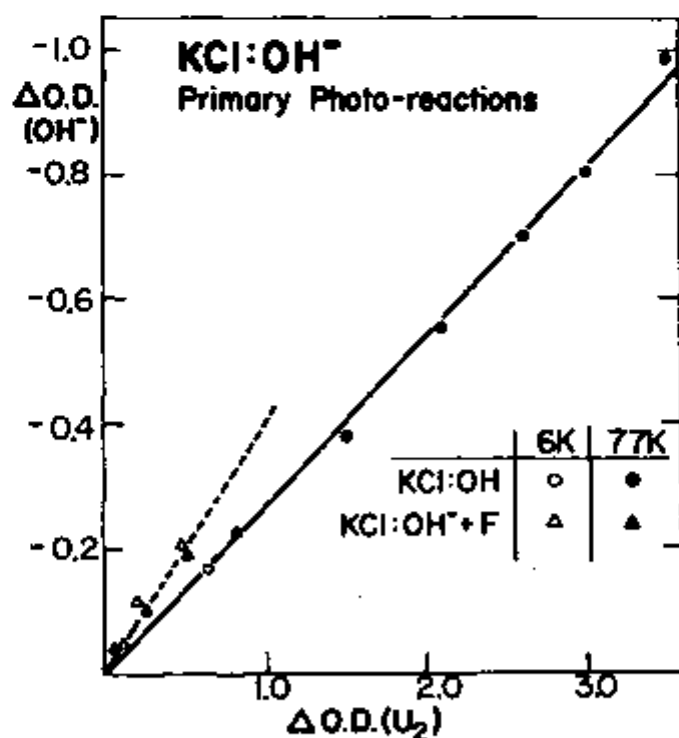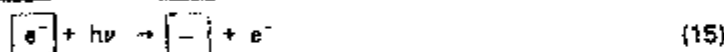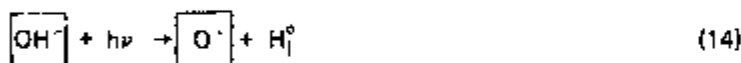

Figure 6 — Plot of the OH⁻ absorption band decrease vs. U_2 band increase at LHe and LN temperature for both systems KCl:OH⁻ (solid line) and KCl:OH⁻ + F (dashed line) obtained during the OH⁻ photodissociation process.

A careful analysis of the number of H_i^o and F centers involved in this process showed that the amount of F center reduced during the OH$^-$ photodissociation process corresponded quantitatively to the difference between the H_i^o centers produced in the two crystals, namely KCl:OH$^-$ and KCl:OH$^-$+F. This indicates that in both cases the same $\boxed{OH^-}$ $\rightarrow H_i^o$ conversion takes place, but that in the presence of F centers part of the created H_i^o centers react with part of the available F centers.

After the observation of these effects an immediate question arises: What is formed out of the H_i^o and F centers which are consumed in this process? Two evident answers may be anticipated: either the created interstitial hydrogen atom, while moving away from the dissociated OH$^-$ state gets captured by a nearby F center, thus creating the H$^-$ center (U band); or an F center ionization takes place in the process and the freed electron will meet a stabilized H_i^o center and form the H$^-$ center (U$_1$ band).

The first possiblity is clearly excluded, because no trace of the (high oscillator strength) U band is observed in this process. The weak and very broad U$_1$ band from H_i^- interstitials is much harder to detect. We could however confirm the presence of the second process by illuminating (after the UV photodissociation) with visible light into the F band (see Figure 4). In doing so, we obtained a further concentration reduction for both F and H_i^o centers (Figure 4). We therefore assume that already, during the UV irradiation, some F centers will be ionized (by irradiation into their conductive states [L bands]) and electrons are transferred to and captured by the H_i^- center, forming H_i^- centers. The observed photochemical reactions to the KCl:OH$^-$+F system can then be summarized by the following equations:

$$\boxed{OH^-} + h\nu \rightarrow \boxed{O^-} + H_i^o \tag{14}$$

$$\boxed{e^-} + h\nu \rightarrow \boxed{-} + e^- \tag{15}$$

$$e^- + H_i^o \rightarrow H_i^- \tag{16}$$

C. THE INTERSTITIAL HYDROGEN ATOM H_i^o (U$_2$ CENTER) AND ITS PHOTO–REACTIONS.

1 — H_i^o photodestruction at LHeT. The electronic absorption of the H_i^o center in KCl consists of a single band (U$_2$ band) peaking at 236 nm. Like the OH$^-$ band for KCl, this band is structureless and asymmetric (halfwidth about 0.40 eV) and its oscillator strength is of the order of 0.33, calculated from the linear correlation of Figure 6 (see Table II). The photo-dissociation of the H_i^o at LHeT is spectrally shown in Figure 7. Similar to the OH$^-$ photodissociation process we obtain by irradiation at LHeT into the U$_2$ band, its decrease accompanied by the appearance of two other bands, the U band (H$^-$ center) and the H band (Cl$_i^o$ crowdion).

The simultaneous creation of U and H bands strongly indicates that the hydrogen atom occupies the vacancy left by the halogen atom during the excitation. This process can be represented by the following equation:

$$\boxed{Cl^-} + H_i^o + h\nu \rightarrow \boxed{H^-} + Cl_i^o \tag{17}$$

The H_i^o centers generated by the photo-dissociation of OH$^-$ defects are isolated and unperturbed interstitial hydrogen atoms which have been extensively studied by EPR and ENDOR techniques in several alkali halides[60,61,62,63]. (See Figure 8A). H_i^o centers can also be produced either by irradiation into the U$_1$ band of H$_i^-$ defects[16] or by the photodissociation of any molecule of the form XH$^-$ (like SH$^-$[64,65]), X standing for an element of group VI. In a model proposed by Kerkoff, et al[57], the H_i^o center can be described by a tetrahedral HCl$_4^-$ molecular ion in which one positive hole in its ground state is mainly bound to the interstitial hydrogen atom (Figure 8A). This ground state hole gives rise to the spin resonance. In the U$_2$ band optical transition to the excited state, a charge transfer mechanism brings one electron of the four surrounding chlorine ions into the hydrogen atom (Figure 8B). Therefore the unrelaxed excited state of the H_i^o center will correpond to a configuration where the hole is more bound to the four surrounding halogen ions and consequently less localized (Figure 8B).
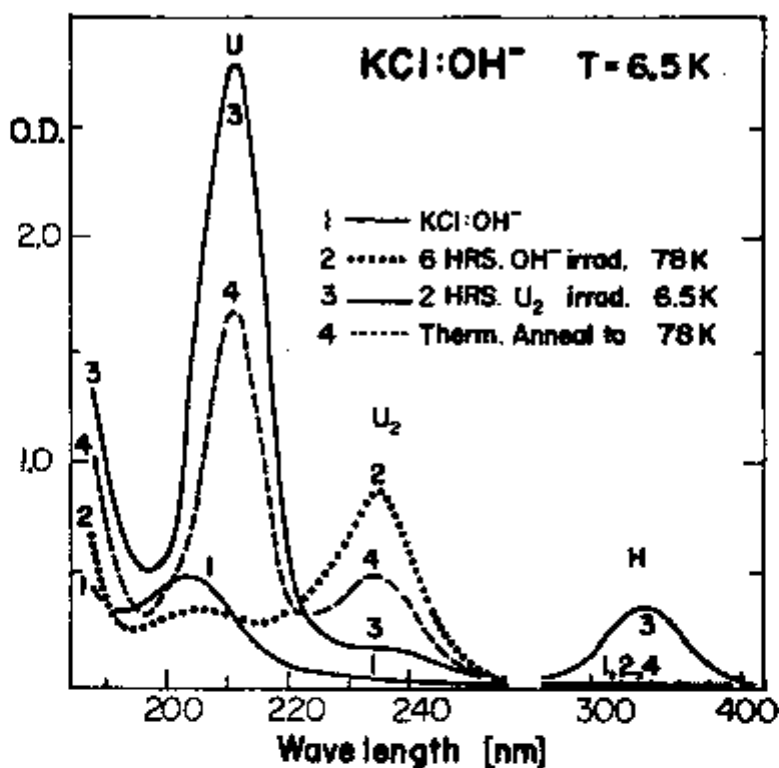
Figure 7 — U_2 center photodestruction spectra at 6.5K and subsequent pulse anneal to 77K, measured at 6.5K.
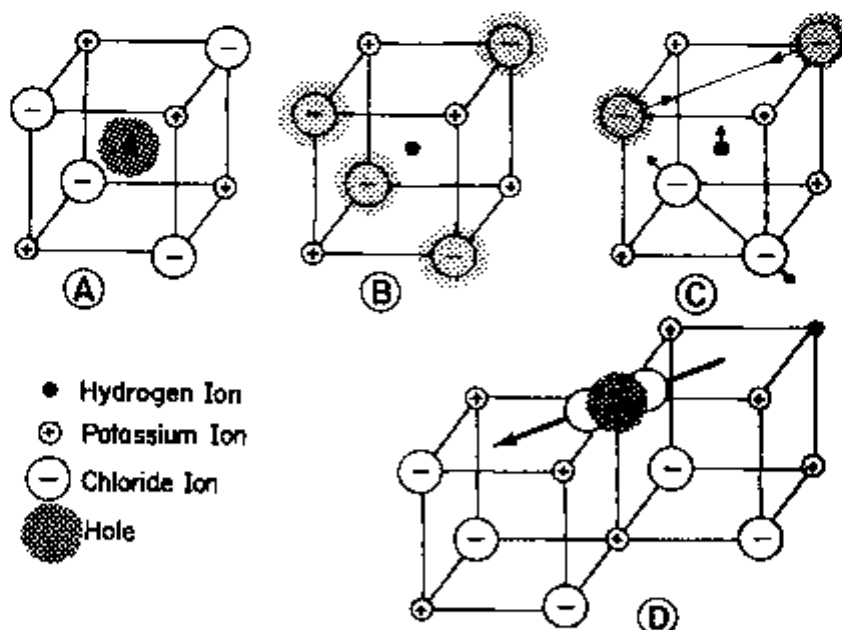

Figure 8A — H_i^o center ground state (the hole is bound to the H^- ion).

    B — H_i^o center unrelaxed excited state after the charge transfer (the hole is shared equally by the four Cl^- ions).

    C — Lattice relaxation and the Jahn-Teller distortion (the hole becomes more localized at the two Cl^- ions which approach each other).

    D — Formation of an H^- center with the creation of a Cl_i^o crowdion moving in a $\langle 110 \rangle$ replacement sequence.

Kurz[120] suggested that In this excited state the lattice will undergo a non-cubic relaxation process (static Jahn-Teller distortion, Figure 8C) after the H_i^o center excitation takes place. This non-cubic lattice relaxation will lower the symmetry possibly displacing the hydrogen ion in the <100> direction and moving chlorine ions in the <110> directions. A polarization of the charge distribution will also take place changing the potential experienced by the hydrogen. The hole will tend to become more localized at the two chlorine ions which approach each other. Annihilation between the transferred electron and the hole may occur restoring the original H_i^o center configuration. Experimentally, however, one observes the H_i^o center photodestruction (with a quantum efficiency which is not yet determined quantitatively). This fact will require some finite escape probability for one of the Cl atoms. Its vacancy will be occupied by the hydrogen ion forming a H^- center. The halogen atom will escape in a <110> collision replacement sequence until it is well separated from the vacancy (hydrogen) left behind and stabilized as a Cl_i^o crowdion (H band), as seen in Figure 8D

A more quantitative approach to the H_i^o photodestruction leads us to Figure 9A where we show the changes in the height of the U_2, H and U bands as a function of the monochromatic U_2 band light irradiation at 6K. Plotting the formed reaction products (H^- and Cl_i^o centers) against the destroyed H_i^o centers, we obtain straight lines (Figure 9B). This is consistent with the assumption that the H_i^o centers decomposition proceeds in a one-to-one ratio to form both H^- and Cl_i^o centers (Equation 17). In this picture, the differences in slope are due to differences in oscillator strengths and halfwidths of the two bands. From these slopes the relative oscillator strengths of the U_2, U and H absorptions can be determined (see Table II).
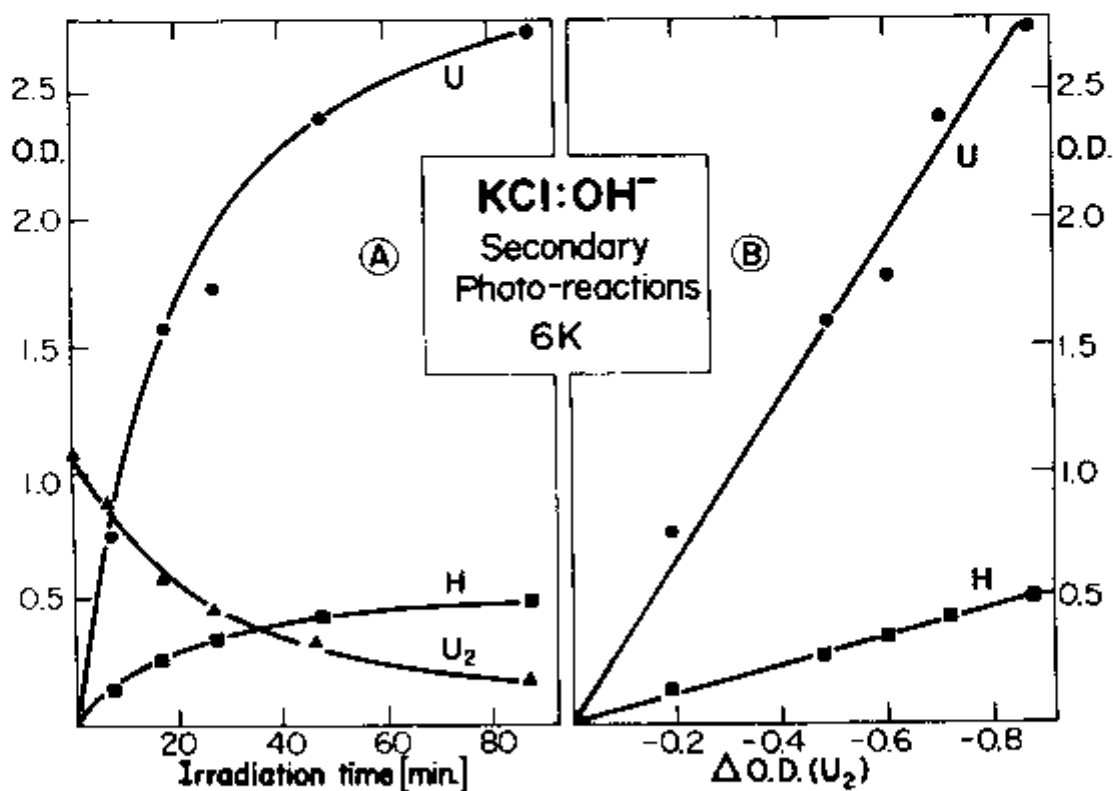

Figure 9 — Photodecomposition of U_2 centers at 6K.

A — Decrease of the U_2-band absorption and increase of the U- and H-band absorption as a function of irradiation time (monochromatic 235 nm light).

B — The U- and H-band increase plotted as a function of the U_2-band decrease, yielding linear Correlations.

As previously reported by Kurz[20], we also observed that the U band produced in this way has a larger halfwidth compared to its normal shape in KCl:H$^-$ crystals. This is apparently due to a close spacing between H$^-$ centers and Cl$_i^o$ crowdions introducing a perturbation in the H$^-$ absorption band. The formation of H$^-$/Cl$_i^o$ pairs is very similar to the conversion of H$^-$ defect into H$_i^-$ and anion vacancies (α-centers)[8] where one also observes different separations between H$_i^-$ and $-$ centers. In both cases one observes a stepwise annealing curve which indicates different thermal stabilities for the different spatial distribution of pairs. A typical H-band annealing curve is shown later in Figure 22. The first step (as described earlier by Delbecq[16]) corresponds to the Cl$_i^o$ crowdion reorientation (around 10K). This reorientation process apparently initiates the recombination of the closest separated H$^-$/Cl$_i^o$ pairs. The widely separated pairs will recombine at somewhat higher temperature (around 50K) through a broader step as is shown in Figure 22. In both cases, these recombinations tend to re-establish the previous H$_i^o$ center which was dissociated into an interstitial halogen atom and a H$^-$ center occupying the original halogen ion position.

After the thermal destruction of all Cl$_i^o$ crowdions (monitored by the complete extinction of the H band), we observed that the process described by Equation 17 has not been completely reversed. This is clearly shown in Figure 7 which contains the final balance between U and U$_2$ bands after the complete H center destruction by annealing to 77K was made (Figure 7). Considering the ratio between the amounts of H$^-$ defects consumed in this back process and the amount of H$_i^o$ centers returned, we get the same value obtained in the production process described by Equation 17. This indicates that apparently no H$^-$ or H$_i^o$ centers were involved in other reactions during the annealing procedure. Nevertheless, the ratio between Cl$_i^o$ crowdions consumed and H$_i^o$ centers returned is much higher than in the crowdion production process indicating that part of the Cl$_i^o$ crowdions during thermal annealing did not make this same back process but must have been trapped and stabilized somewhere else in some other form. However, no new absorptions were observed to develop in the whole UV and visible region of the spectrum. The question, into what structures the mobile Cl$_i^o$ crowdions become trapped and stabilized, remains open and unanswered at this point.

2 – H$_i^o$ Photodestruction at LNT. Irradiation into the U$_2$ band at LNT leads to spectral changes very similar to the ones obtained in the above discussed case of LHeT irradiation: The U$_2$ band is reduced and the U band is formed (Figure 10). No H band is formed as expected from the fact that the Cl$_i^o$ crowdions are no longer stable at LNT. If we plot – similarly as for the LHeT case in Figure 9 – the U$_2$ and U band changes against irradiation time (Figure 11A) and compare the increase of the U band with the U$_2$ band decrease (Figure 11B) we find, in comparison to the LHeT behavior, the following changes:

a) The initial quantum efficiency for the optical H$_i^o$ center destruction is about ten times smaller than it was at LHeT (Figure 11A).

b) Though a linear relation between U$_2$ band decrease and U band increase is again obtained (Figure 11B), their ratio is different from the one obtained at LHeT.

Point (a) shows phenomenologically that the stability of the H$_i^o$ center against optical bleaching is considerably higher than at LHeT. If we assume that the initial photodestruction of the H$_i^o$ center produces the Cl$_i^o$ crowdion center (as it does at LHeT), this thermally unstable interstitial center may easily recombine back and restore the initial H$_i^o$ center. This would account for the low efficiency of the H$_i^o$ center photodestruction.

Still in 10% of the U$_2$-band excitation cases (compared to LHeT), the H$_i^o$ photodestruction works and U centers are formed. This means that the mobile Cl$_i^o$ crowdion did escape without recombination and must get trapped and stabilized at some unknown place, undetectable with UV and visible spectroscopy. The fact that in this process the $|\Delta U|:|\Delta U_2|$ ratio is different from the 1:1 ratio found at LHeT as indicated in point (b) suggests that hydrogen in some form may be involved in the stabilization and trapping of the Cl$_i^o$ crowdion.
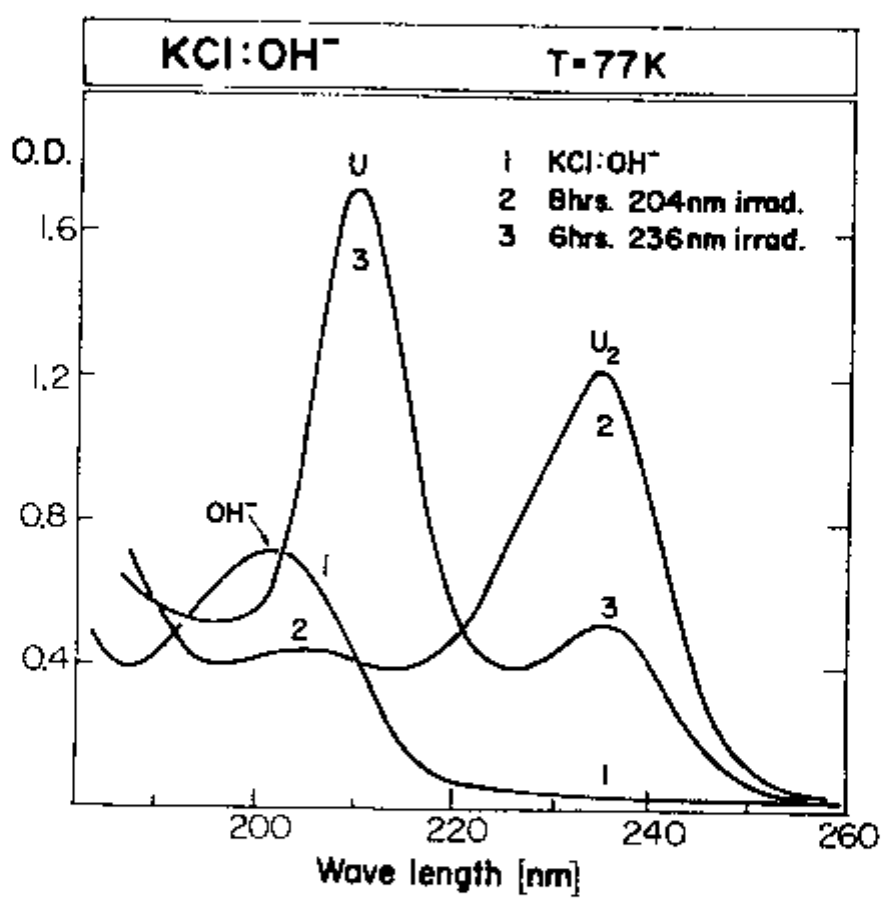
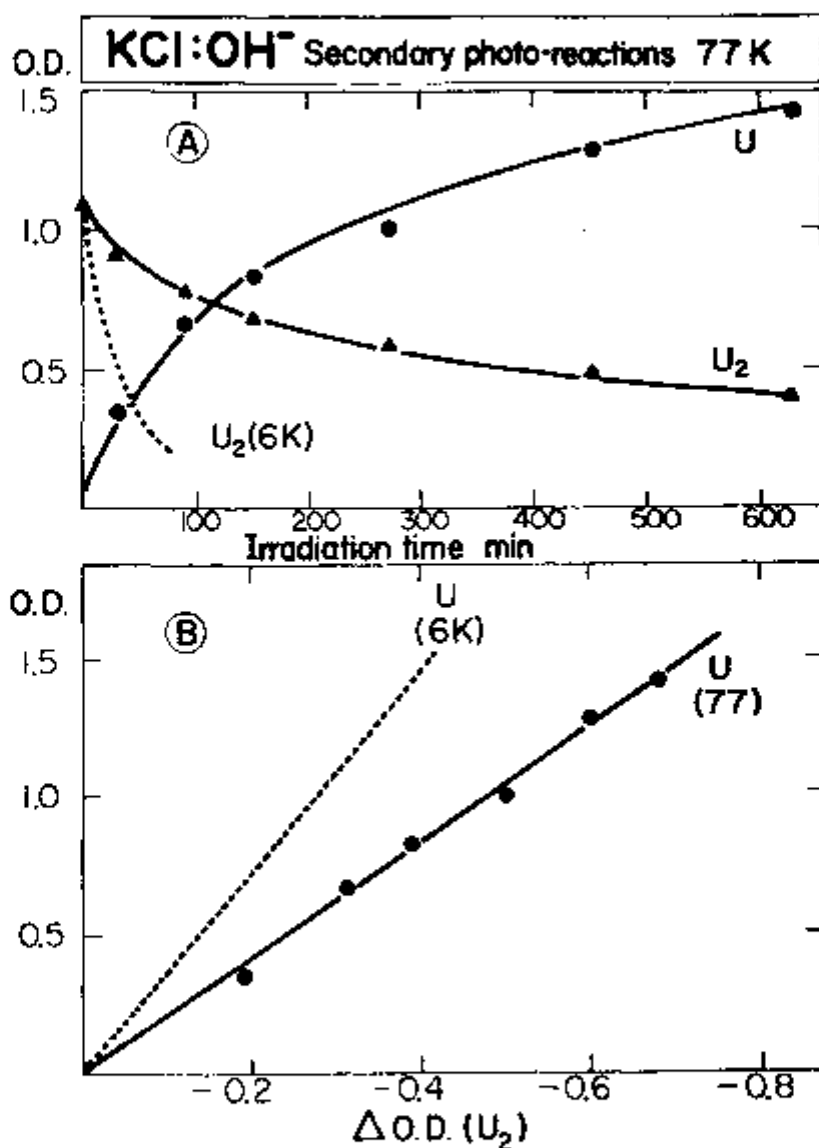**Figure 10** — Photodissociation of OH⁻ centers (1→2) and subsequent H_i^0 center photodestruction (2→3), at 77K.

Figure 11 — Photodecomposition of U_2 centers at 77K.
A — Decrease of the U_2-band absorption and increase of the U band absorption. The dashed line indicates the initial rate obtained at 6K.
B — The U-band increase plotted as a function of the U_2 band decrease. The dashed line indicates the same reaction at 6K, corrected for the broadening effect on the perturbed H⁻ centers.

The precondition for this line of arguing is the assumption that the photoexcitation of the H_i^o center at LNT leads — similar to the LHeT case — primarily and initially to the formation of a Cl_i^o crowdion — even if it is thermally not stable and therefore not detectable by the H-band. How can we prove experimentally that this assumption is true? Simply by offering the Cl_i^o crowdions a trap that would thermally stabilize them. This can be achieved by additonally introducing Na^+ impurities in KCl:OH⁻ systems. Cl_i^o centers trapped in the immediate vicinity of a single substitutional Na^+ impurity are called H_A centers (or formerly, before the clarification of their structural model, V_1 centers)[37].

H_A centers in KCl give rise to a strong transition at 357 nm and a weaker one at 560 nm. These H_A bands have a thermal decay temperature of about 113K. We repeated with a KCl:Na⁺ + OH⁻crystal at 77K the same previously described sequence of monochromatic irradiations starting with the OH⁻ photodissociation, followed by the U_2 band photodestruction. The results are displayed in Figure 12. As we can see from there, we were able to produce H centers and have them trapped at Na^+ impuritles and stabilized at 77K. This process can be described by the following equation:
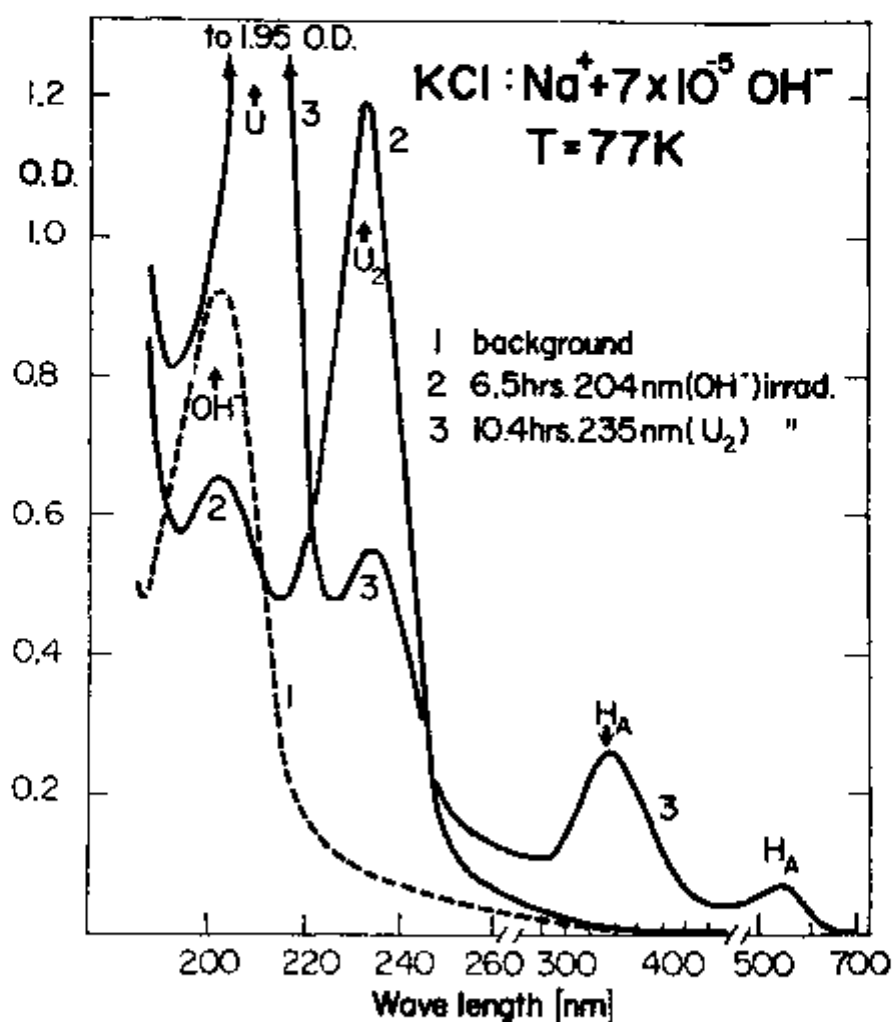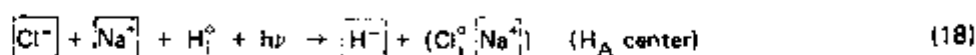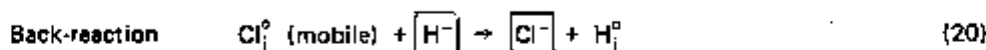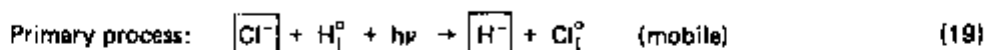
$$\boxed{Cl^-} + \boxed{Na^+} + H_i^o + h\nu \rightarrow \boxed{H^-} + (Cl_i^o \boxed{Na_s^+}) \quad (H_A \text{ center}) \tag{18}$$

Figure 12 — H_A center formation in a KCl:OH⁻ + Na⁺ crystal under U_2 light irradiation at LNT.

These experiments show clearly that photoexcitation of H_i^o centers at LNT leads (similar to the LHeT case) to the production of Cl_i^o crowdions. The difference to the low temperature case is that these crowdions are thermally unstable and mobile (i.e., don't appear by the H band absorption). They either recombine with the U center and restore the initial H_i^o defect, or escape in the lattice looking for a different trapping site. In a Na^+ doped crystal they can be trapped by a Na^+ ion, forming the thermally stable H_A (Na^+) configuration.

We can therefore assume that in our crystal with oxygen and various hydrogen defects a different trapping place is operative, which can stabilize the mobile Cl_i^o crowdion and therefore allows even at LNT the $H_i^o \rightarrow$ H^- conversion. Thus we must have at LNT reactions of the type:

Primary process: $\boxed{Cl^-} + H_i^o + h\nu \rightarrow \boxed{H^-} + Cl_i^o$ (mobile)   (19)

Back-reaction Cl_i^o (mobile) $+ \boxed{H^-} \rightarrow \boxed{Cl^-} + H_i^o$ (20)

Escape-reaction: Cl_i^o (mobile) $+ X_{trap} \rightarrow (Cl_i^o X_{trap})$ (21)

The same X_{trap} would have been responsible for the unaccounted disappearance of Cl_i^o crowdions in the thermal annealing process after their production at LHeT, treated before. In both cases, no UV or visible absorption has been found to identify the $(Cl_i^o X_{trap})$ complex. As hydrogen in some form is a candidate for the X_{trap}, we set up IR experiments with the aim to possibly identify the trapped Cl_i^o crowdion by local mode spectroscopy.

D. THE NEW H_x^- CENTER.

1 – Photo-production at LNT with monochromatic light. To investigate all the transparent range of the crystal with UV, Vis and IR spectroscopy — especially in the hydrogen center local mode region — we set up two experiments with the two parallel and perpendicular geometries (described in Chapter III) using crystals of suitable dimensions (see Figure 13). The aim was to produce the same photochemical reactions in both samples in parallel so we could carefully detect and correlate any IR effects to the already known spectral behavior in the UV region.

As one can see in Figure 13A, we started with the photodecomposition of the OH^- defect by monochromatic 204 nm irradiation As a result we observed in the UV range the $\boxed{OH^-} \rightarrow H_i^o$ conversion as described earlier. In the IR range no significant spectral changes can be observed at this stage, as expected. The OH^- stretching vibration absorption at 2.7μ is too weak to be detectable for the low OH^- doping used, and the neutral H_i^o interstitial does not give rise to an optical active local mode. In the next step we photo-destroyed H_i^o centers, reproducing our former UV spectral results. In this irradiation stage, pronounced effects developed in the IR range. Besides the appearance of the H^- local mode transitions — as expected from the UV result — we observed the growth of a new single band so far not reported in the literature. This band has its maximum at 1112 cm^{-1} (at LNT), at a 30% higher energy compared to the H_i^- center local mode transition. We call the center responsible for this new hydrogen local mode absorption tentatively H_x^-, with the "x" indicating its unknown structure and site, and the minus sign indicating that this new center should be charged to be IR active.

Proceeding with the series of spectral irradiations in Figure 13, we illuminated in the third stage with U-band light, producing the well known $\boxed{H^-} \rightarrow H_i^-$ conversion. This step basically did not change the optical density of this new center. As expected we observed in both ranges (IR and UV) the decrease of the H^- center (U band) and besides the increase of the H^- center, the U band destruction is also responsible for some H_i^o /F center pairs formation. The new H_x^- defect apparently does participate in all these transformations.
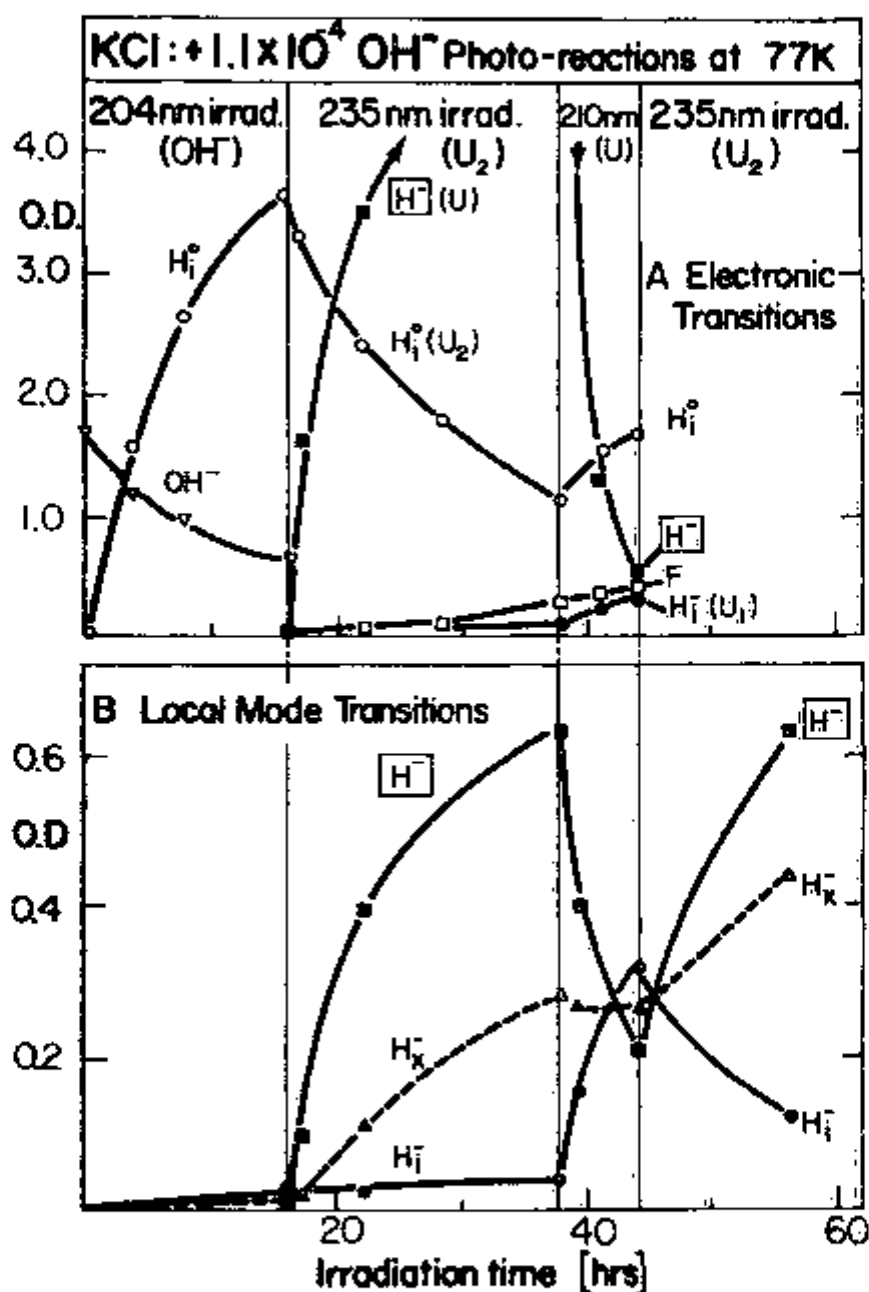
Figure 13 A — Electronic absorption bands as a function of irradiation time for a sequence of monochromatic irradiations in a KCL:OH⁻ crystal at LNT (thickness ~ 0.5 mm).

B — Local mode transitions in the IR for the same sequence of irradiations as in A (thickness ~ 8.0 mm)

A further U_2 band irradiation was performed in the case B, mostly to follow in the IR the behavior of the new H_X^- band. The major effects after this irradiation were the increase of the H^- center, the increase of the H_B^- band and a decrease of the H_i^- centers. A decrease of the H_i^- center could partially be explained by the fact that U_2 band irradiation also reaches the U_i electronic absorption band which is very broad and extends from 280 to 230 nm in the far UV.

We should point out here that in a similar set of experiments with a KCl:OH$^-$+ Na$^+$ crystal, the monochromatic U_2 band irradiation only brought up H_A centers as mentioned before (shown in Figure 12) with no traces of H_X^- center formation in the IR region.

2 — Photoproduction at LNT with undispersed irradiation. Some preliminary questions immediately arise concerning the H_X^- center: How does the crystal behave under a prolonged full undispersed UV exposure when all possible photochemical reactions were taking place simultaneously and are performed to complete saturation? To answer this question we set up the following experiment: Utilizing an irradiation system which has a Xenon lamp as a light source, we performed a full undispersed irradiation experiment for KCl samples of two different concentrations of OH$^-$. For the low OH$^-$ concentration sample we observed a parallel rise of the H_i^-, H_i^- and H_X^- center transitions (Figure 14A). After a prolonged irradiation these transition bands reached some sort of dynamical equilibrium and saturated. In several attempts we disturbed this dynamical equilibrium by illumination with monochromatic light into the U band for example, producing the $\boxed{H_i^-} \rightarrow H_i^o + \boxed{-}$ conversion already described in Figure 13B. Conversely we would invert this process by illuminating into the U_1 band. While the relative amounts of H^- and H_i^- local mode absorptions changed reversibly in these tests, the height of the H_X^- transition band remained approximately constant (as it did in the experiment shown in Figure 13B). At the end we were able to return to the dynamical equilibrium relative heights of these three transitions as shown in Figure 14A just by repeating for a few hours the full Xenon lamp irradiation. The IR local mode transitions and the corresponding UV spectral absorptions after ten hours of undispersed light irradiation are shown respectively in Figures 15A and 15B. From the UV spectrum we can confirm that no new bands were found in the UV region. This is consistent with the fact that the H_X^-, apparently having no significant electronic transition in the transparent crystal range, will be the most prominent product of the OH$^-$ photodecomposition at LNT, as observed from this saturation experiment.

We repeated this full Xenon lamp irradiation experiment for a KCl:OH$^-$+ Na$^+$ sample (see Figure 14B) and observed the same saturation behavior as the one obtained with a KCl:OH$^-$ sample (Figure 14A). Since our irradiation also contains the wavelength which is absorbed by the H_A centers, this kind of undispersed irradiation prevents their formation. (We confirmed the photodestruction of H_A centers in another experiment where we bleached the H_A band by irradiating monochromatic light that is absorbed by the H_A center.) As a result of this saturation experiment we again ended up with H_X^- centers as the most prominent band.

For a higher concentrated KCl:OH$^-$ sample, under the same initial build-up of these three transition bands (Figure 16). The initial build-up of these transition bands (Figure 16). The initial formation rate of the H^- centers is low, but increases markedly under prolonged irradiation. This means that under undispersed irradiation conditions the H^- transition band is formed at the expense of another reaction product which must be initially created by the light irradiation.

3 — H_X^- local mode spectra and isotope effect. H_X^- formation in KBr:OH$^-$ and RbBr:OH$^-$ crystals. A closer look at the H_X^- transition band revealed very interesting features. It did not show any structure or splitting when cooled to low temperatures, displaying a single band with maximum at 1114 cm^{-1} and a halfwidth of 2,5 cm^{-1} at 6K. The variation of the band shape as a function of temperature can be seen in Figure 17.

Our general observations on the H^- center so far strongly indicate the presence of a hydrogen. But how would one confirm the presence of a hydrogen in this new defect? A rather straightforward test was to repeat the full Xenon lamp irradiation for a system such as KCl:OD$^-$ and search for isotope shifts in the

observed transitions. This experiment is described in Figure 18. We indeed observed the displacement of the H_x^- transition from 1112 to 779 cm^{-1}, an almost perfect $\sqrt{2}$ isotope shift (H→D). Parallel to this we also observed the isotope shift for the local mode of the H$^-$ center from 845 cm^{-1} to 606 cm^{-1}.

Finally, in a brief attempt to demonstrate the generality of the H_x^- defect and its photoproduction from OH$^-$ defects, we took KBr:OH$^-$ and RbBr:OH$^-$ samples and repeated the full Xenon lamp irradiation experiment. We indeed found in these two systems the formation of H_x^- and H_i^- centers as in the KCl:OH$^-$ system. For KBr:OH$^-$ the peak positions of H_x^- and H_i^- were 1095 cm^{-1} and 790 cm^{-1} respectively. For RbBr:OH$^-$ they were 1021 cm^{-1} and 745 cm^{-1} respectively. These results indicate the general nature of the H$^-$ center excluding the possibility of its being formed only in KCl:OH$^-$ systems.
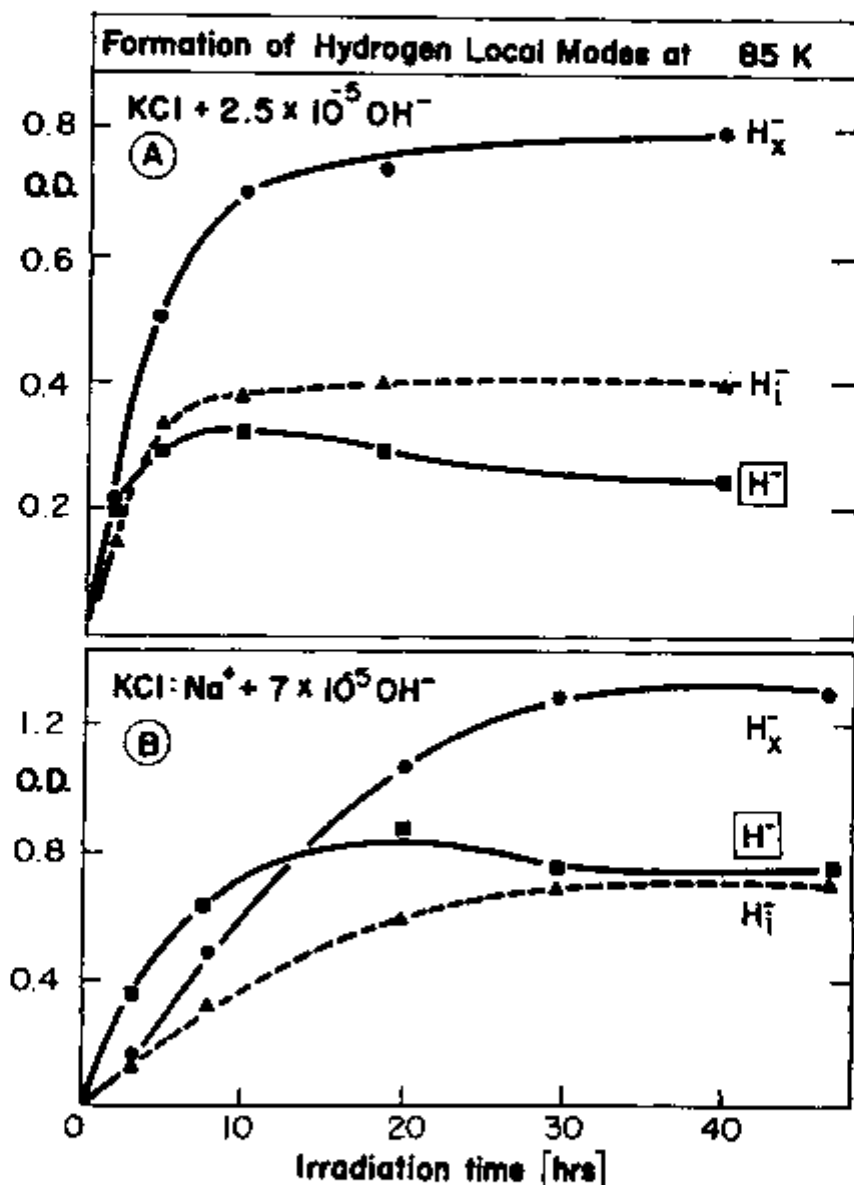

Figure 14 — Plot of the local mode transitions of H$^-$, H_i^- and H_x^- centers as a function of irradiation time under full Xenon lamp irradiation at 85K (measured at 77K).

A — KCl:OH$^-$ system.
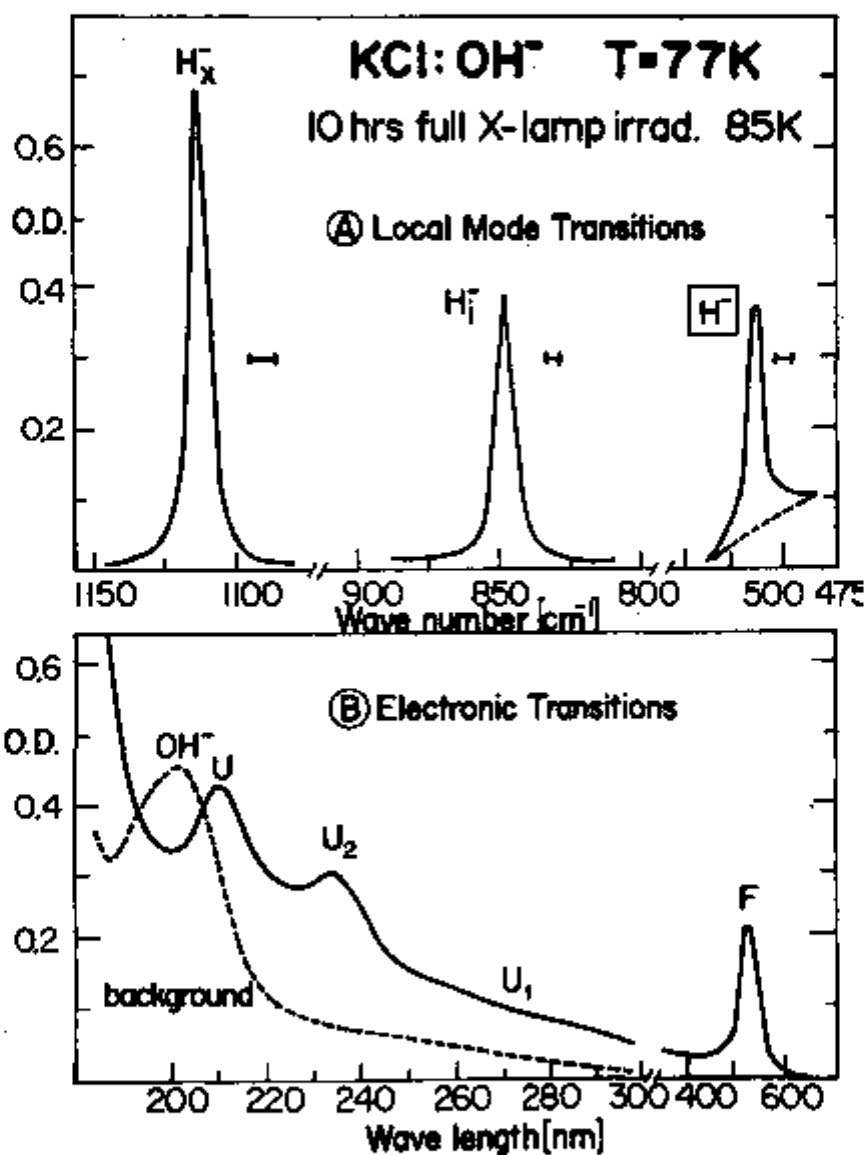
B — KCl:OH$^-$ + Na$^+$ system.

Figure 15 A — Hydrogen centers local mode transitions after 10 hours of full Xenon lamp irradiation at 85K (measured at 77K).
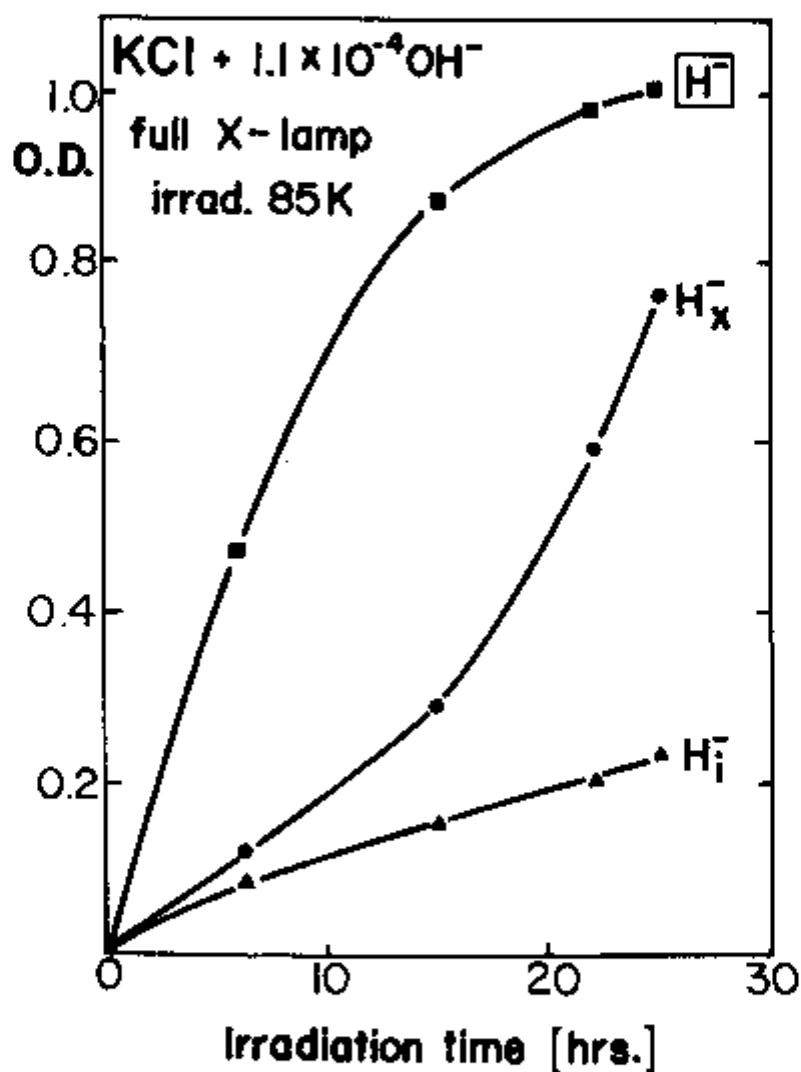
B — The respective UV spectra.

Figure 16 — Plot of the local mode transitions of H^-, H_i^- and H_x^- centers as a function of irradiation time under full Xenon lamp irradiation for a KCl:OH$^-$ crystal with higher OH$^-$ concentration.
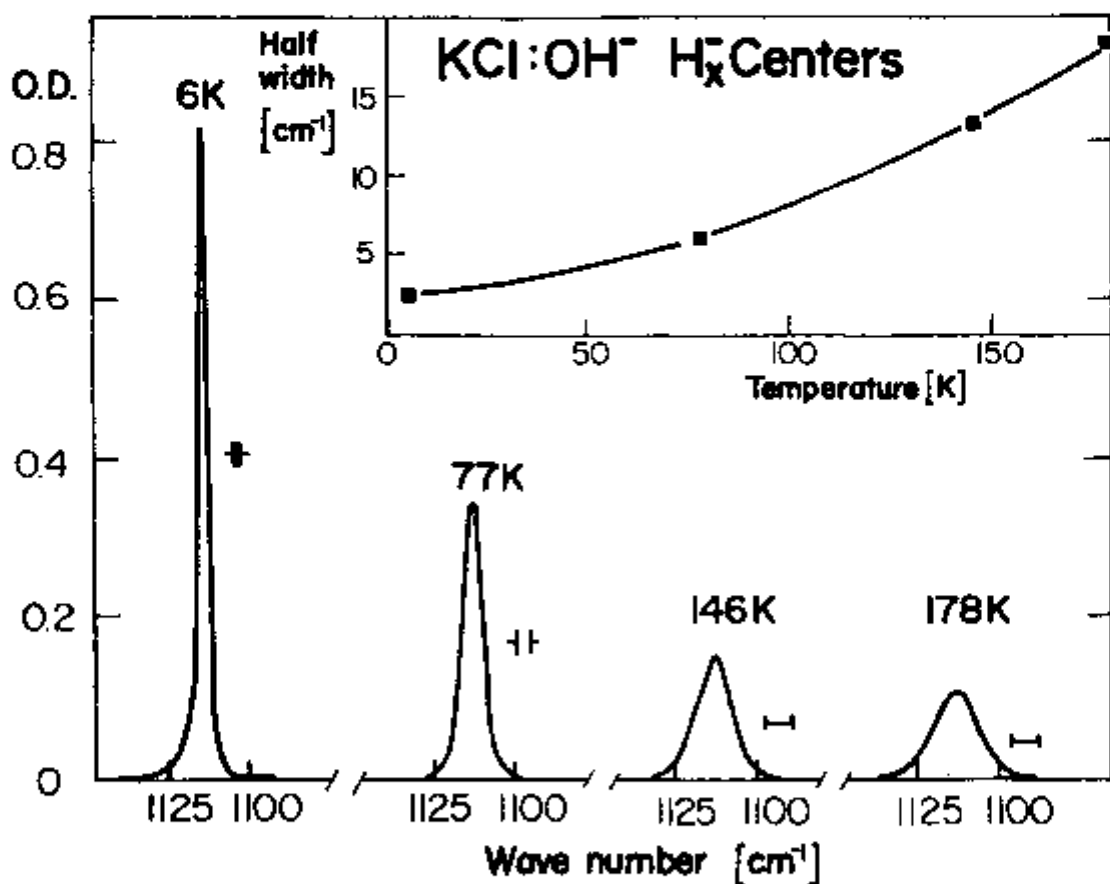
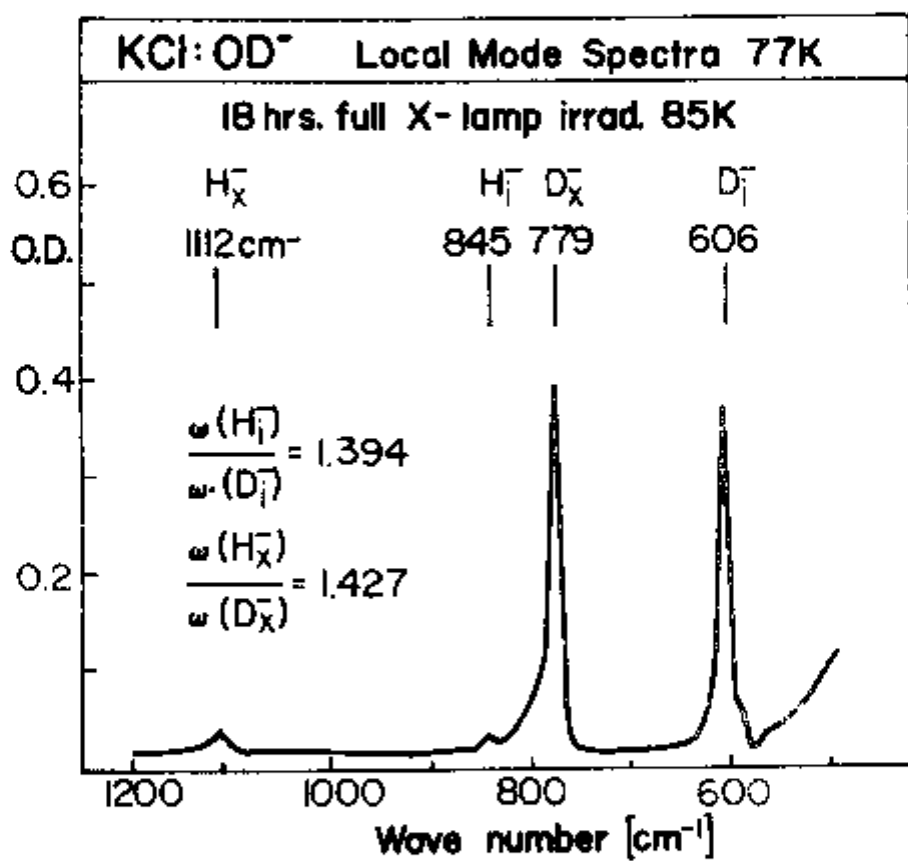Figure 17 — Temperature dependence of the spectral shape and halfwidth of the H_x^- local mode transition

Figure 18 — Isotope shift effects of the H_x^- and H_i^- in a KCl:OD$^-$ crystal after full Xenon lamp irradiation at 85K (measured at 77K).

32

Up to this point we know or anticipate that hydrogen and mobile Cl_i^o crowdions are the basic candidates for the formation of the H_x^- band. However we must remember that so far we only dealt with one of the two products of the OH^- photodissociation, namely the H_i^o center. In other words, the O^- center was never taken into consideration although it was always present and in the same quantities as the initaial H_i^o center.

In the full irradiation experiments, the presence of the O^- center is even more critical since here we are also irradiating in the O^- band. This could result in photochemical reactions involving the O^- center and consenquently the production of new defect aggregations.

Since the precise optical detection of the O^- center and its contribution in the various defect reactions experimentally impractical, its exclusion from the formation of the H_x^- center can only be proven by indirect experiments. How would we then, at the same time, create crowdions, have hydrogen traps for these crowdions, and avoid the undesirable presence of the O^- center?

4 – The formation of H^- centers in KCl:H$^-$ crystals.

a) X-irradiation of KCl:H$^-$ at LNT.

At this point the most obvious experiment to answer the preceding question was to X-irradiate a KCl:H$^-$ system at 77K. The reasons to do so are:

(i) X-rays are well known to produce Cl_i^o crowdions in KCl at low temperatures[66].

(ii) A KCl:H$^-$ system would offer hydrogen traps for the mobile crowdions.

(iii) A KCl:H$^-$ system would exclude the presence of the O^- centers.

We X-irradiated a KCl sample containing 5.6×10^{-5} H$^-$. Due to the high concentration of H$^-$ defects, its local mode transition was monitored by the anti-Stokes phonon side band, since the main local mode transition is completely off scale (by a factor of ~ 40 higher than the phonon side band at LNT[67]).

After a prolonged X-irradiation we observe the formation of structured H_i^- local mode absorptions (Figure 19A). These spectral structures correspond to transitions of H$^-$ centers that have different spatial correlations to their anti-centers – the anion vacancies – as explained by Fritz[18]. The X-irradiation also produces H_x^- centers as we had anticipated (Figure 19A).

In the next Figure 20A we display the growth and decay curves of the centers involved in Figure 19A. We observe that X Irradiation produces the following effects:

(i) H$^-$ centers undergo a gradual reduction, reflected by the decrease of its phonon sideband.

(ii) H_i^- centers measured by the main peak from the spatially uncorrelated ones are formed with an approximately constant rate.

(iii) H_x^- centers are formed initially with a small rate which increases under further X-irradiation.

From (iii) we recognize that H_x^- centers are formed more efficiently with the help of some reaction product that is obtained during the initial X-irradiation exposure. This observation makes the H_i^- center the strongest candidate for a trapping site for the Cl_i^o crowdions.

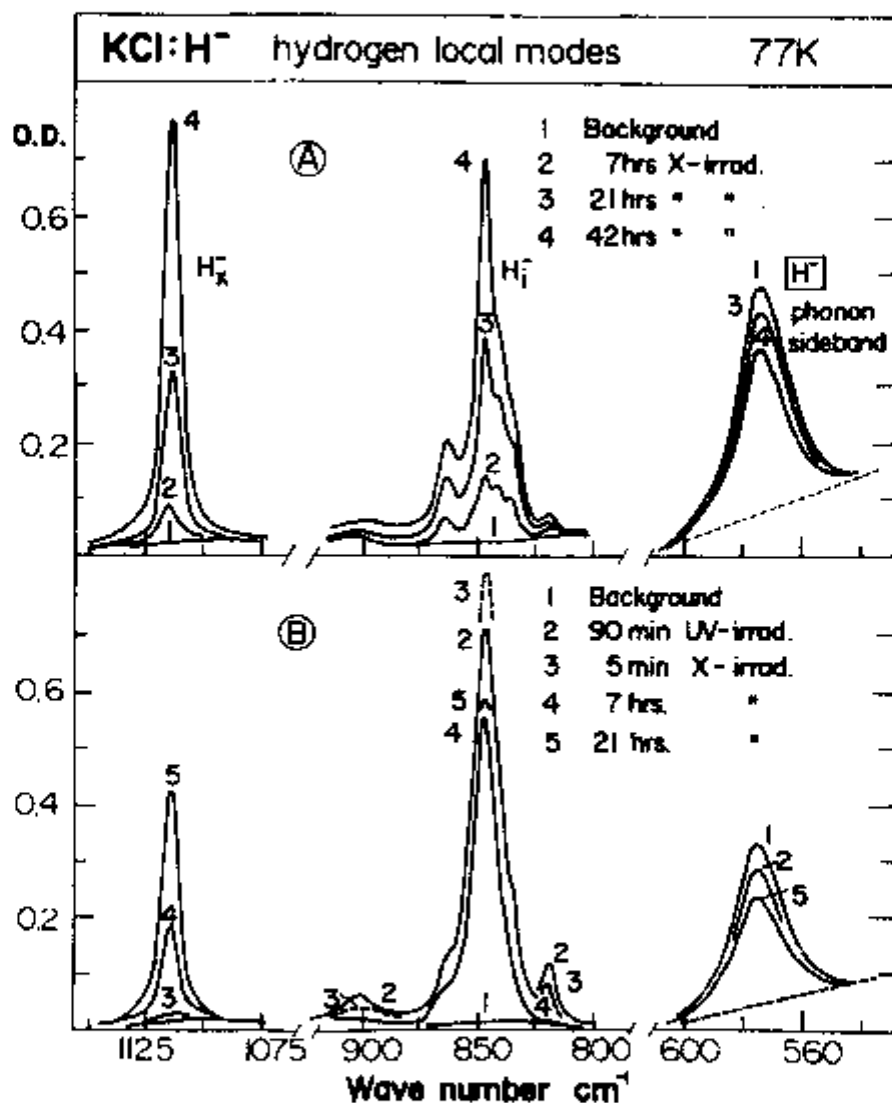**Figure 19 A** — Formation of H_x^- and H_i^- (of different spatial correlations) centers in a KCl + 5.6 × 10^{-5} H^- sample under X-rays irradiation at 77 K.

B — The same as above but after a previous UV irradiation, producing $\boxed{H_i^-}$ → H_i^- conversion.
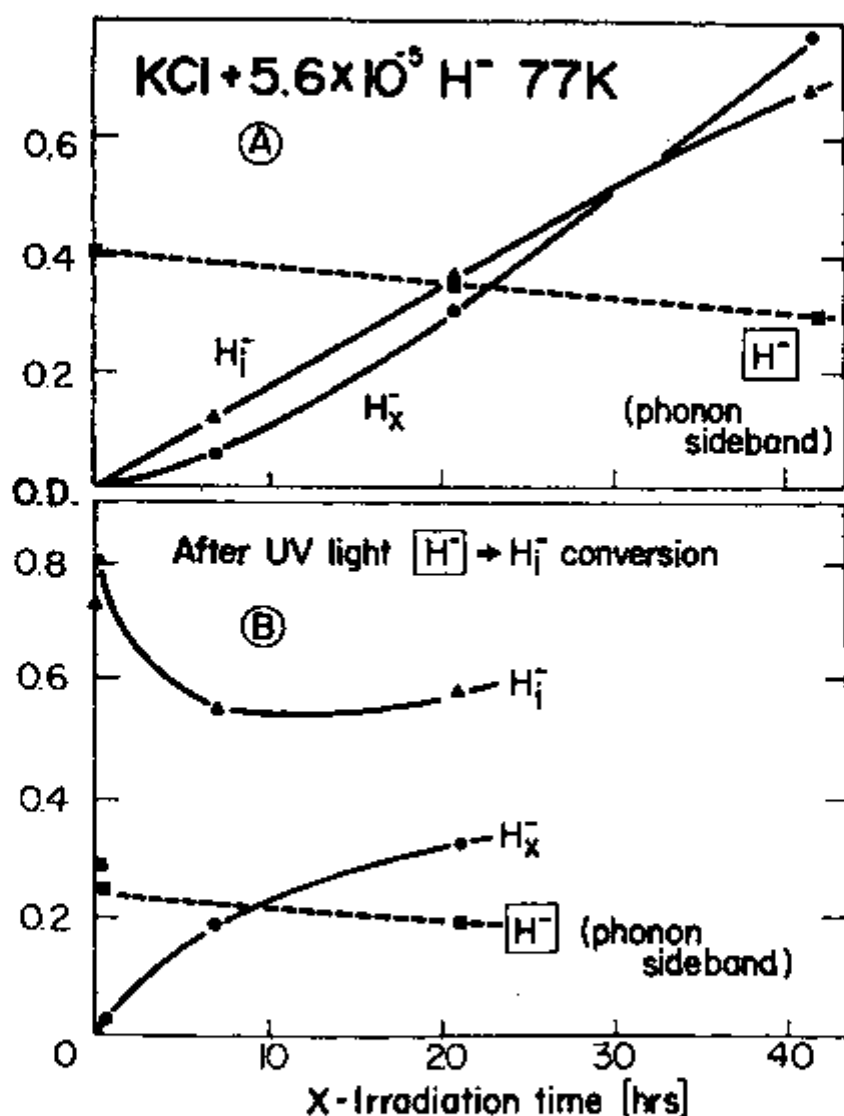
Figure 20 A — Increase of H_x^- and H_i^- (uncorrelated ones) as a function of X irradiation tiem. The consumption of H^- centers is monitored by the phonon sideband of the H^- local mode.

B — The same as above but after the previous UV irradiation. All data are taken from The spectral measurements in Figure 19.

b) X-irradiation after optical $\left[H_i^-\right] \to H_i^-$ conversion.

In order to further verify the participation of H_i^- defects in the H_x^- production process, we set up another experiment in which we pre-exposed a KCl:H$^-$ sample to UV irradiation. As a result of this UV irradiation we obtained, very efficiently, the $\left[H_i^-\right] \to H_i^-$ conversion process without any trace of H_x^- center formation (see Figure 19B).

Under X-irradiation of this previously UV exposed sample, we observed an initial decrease of H_i^- centers and an increase of H_x^- centers with an initial formation rate a factor of ~ 16 larger than the initial H_i^o formation rate obtained by a direct comparison of Figure 20A with Figure 20B. Under further X-ray exposure the system tends to reach some dynamical equilibrium. The observed facts confirm again strongly the pronounced participation of the H_i^- center as a trapping site for the Cl_i^o crowdion. We cannot decide from these experiments if H^- defects play any role as the Cl_i^o crowdion traps. We can, however, conclude that if they participate in the formation process, this trapping probability for Cl_i^o crowdion is considerably lower than that of H_i^- defects.

A doubt that emerges after doing these X-ray experiments may be expressed by the following question: Could the KCl:H$^-$ sample contain unwanted OH$^-$ impurities which would have produced the H_x^- effects under X-irradiation? Due to the high concentration of the H$^-$ center, their UV absorption would completely mask any small OH$^-$ band. Two conclusive arguments can be given against such a possibility:

(i) The same UV light exposure which formed no H_x^- centers in the experiment of Figure 19B produced, in experiment shown in Figure 13A an optical density of 0.15 in the H_x^- local mode absorption. If our KCl:H$^-$ sample of experiment Figure 19B would have a factor of six lower concentration of OH$^-$ impurity than experiment Figure 13A, we should have been able to produce 0.02 O.D. of H_x^- local mode absorption (0.02 O.D. was the lower limit of our detection system ability at the signal-to-noise ratio used). We can therefore say that if OH$^-$ was present in the KCl:H$^-$ sample it should be in concentrations less than 4×10^{-6}.

(ii) In another experiment we exposed a sample of low OH$^-$ concentration (2.5×10^{-5}) to X-rays at LNT during 16 hours and were unable to find any trace of H_x^-, H_i^- or H^- centers. This shows that X irradiation at LNT does not decompose at all the OH$^-$ defect into any of the hydrogen reaction products H^-, H_i^- and H_x^- as observed under UV irradiation of OH$^-$. The participation of any unwanted OH$^-$ additions in the experiments of Figures 19 and 20 is therefore definitely excluded, and so is the possible participation of any oxygen defects in the H_x^- formation.

For a further confirmation of the non-participation of the O$^-$ center in the H_x^- center formation we did another experiment in which we used a KCl:SH$^-$ crystal and repeated the full UV irradiation treatment as we did with the KCl:OH$^-$ crystal. We know from previous work[64,65] that the SH$^-$ center can be decomposed into S$^-$ and H_i^o defects. Proceeding with this full irradiation treatment we observed exactly the same H_x^- band in the KCl:SH$^-$ crystal.

The experiments described in this section, besides confirming the participation of H_i^- and Cl_i^o centers into the H_x^- center formation, ruled out completely any possibility of the participation of the O$^-$ center in the H_x^- center production.

5 — Conclusions about H_x^- formation from LNT experiments. Up to this point the various experiments at LNT allow us to draw several conclusions about the nature and formation process of the new H_x^- center:

a) Under full UV light irradiation, H_x^- centers are the most prominent hydrogen reaction products of the OH$^-$ photodecomposition.

b) Under stepwise monochromatic OH$^-$ photodecomposition, H_x^- defects form in the secondary stage by photoexcitation of H_i^o centers. As this process creates mobile Cl_i^o crowdions, the latter are very likely candidates for the H_x^- formation.

c) The IR absorption of the H_x^- centers shows, by the H $\rightarrow$ D isotope shift, that it is caused by a perfectly localized vibration of a charged hydrogen ion: its single band structure indicates a site of high symmetry for the hydrogen, which does not split its local mode.

d) H_x^- centers can be formed by X-irradiation of KCl:H$^-$ crystals at LNT. This excludes any contribution of the oxygen in the H_x^- formation process, and confirms the idea that H_x^- centers are formed by the reaction of mobile Cl_i^o crowdions with hydrogen defects. The increase of the initial H_x^- formation rate in this experiment by a previous $|H_i^-\rangle \rightarrow H_i^-$ conversion makes the interstitial H_i^- defect the most likely candidate for the trapping of the Cl_i^o crowdion forming the H_x^- center.

All the preceding experiments were done at LNT, where Cl_i^o crowdions are mobile right after their creation and thus form the H_x^- defects instantanneously.

If this picture is correct, we should be able to produce H_x^- centers in controlled steps at *lower* temperatures where Cl_i^o crowdions are thermally stable. Experiments in this temperature range should therefore provide a conclusive test on the formation process and a definitive identification of the hydrogen defect trapping the Cl_i^o crowdion.

E. CONTROLLED PRODUCTION OF H_x^- CENTER AT LHeT.

1 — Production by monochromatic UV irradiation. We initially made the photo-dissociation of the OH$^-$ center at 77K (for experimental convenience) by monochromatic 204 nm light (Step 0 in Figure 21A). We then proceeded with the further photochemical reactions at 6K. After photodecomposing H_i^o centers (Step 1, Fig. 21) at 6K we observed that the H$^-$ center local mode was built up as expected from previous experiments. In contrast to the corresponding experiment at LNT (see Figure 13), we observe at this step no trace of H_x^- (and H_i^-) formation. This confirms our previous assumption that the photodestroyed H_i^o centers are quantitatively converted into H$^-$ centers and Cl_i^o crowdions, with the latter stabilized as H centers in the lattice. It further confirms our assumption that only mobile Cl_i^o crowdions, reacting with hydrogen defect, are able to form the H_x^- centers. The "self-trapping" of the Cl_i^o crowdions as H centers therefore prevents the H_x^- formation.

If our line of arguing is right, the H_x^- centers should be formed if we make the produced Cl_i^o crowdions mobile in some way. One way to achieve this is the optical excitation in the electronic transition (H band) of the Cl_i^o crowdion, which leads to an optically stimulated motion of the defect. If we shine monochromatic light into the H band (Step 2 in Figure 21), we indeed observe the appearance of the H$^-$ local mode band. Simultaneouly we see the reduction of the H$^-$ local mode band.

As no H_i^- defects have been present during this reaction we must conclude that in this step H_x^- defects have been formed by the reaction of "optically mobilized" Cl_i^o crowdions with H$^-$ defects.

A further irradiation into the U_1 band (Step 3 in Figure 21) proceeds with the $H_i^o \rightarrow H_i^- + Cl_i^o$ formation as in Step 1 without further H_x^- formation. A subsequent monochromatic irradiation in the U band brought up mainly the local mode of the $H_i^-/|I^-\rangle$ close pairs

(Step 4, Figure 21B) with the correspondent decrease of the H⁻ absorption center. Now that we have two kinds of hydrogen centers competing as trapping sites, we again optically bleach the H band and observe further increase of the H_x^- local mode band. Simultaneouly we see a considerable reduction in the local mode absorption of the H_i^-/⊟ close pairs, and a very small reduction in the H⁻ local mode. Apparently when both H⁻ and H_i^-/⊟ pairs are offered are much more effective for the H_x^- formation. This is exactly what we observed in the X-ray experiment with the KCI:H⁻ crystals of LNT.
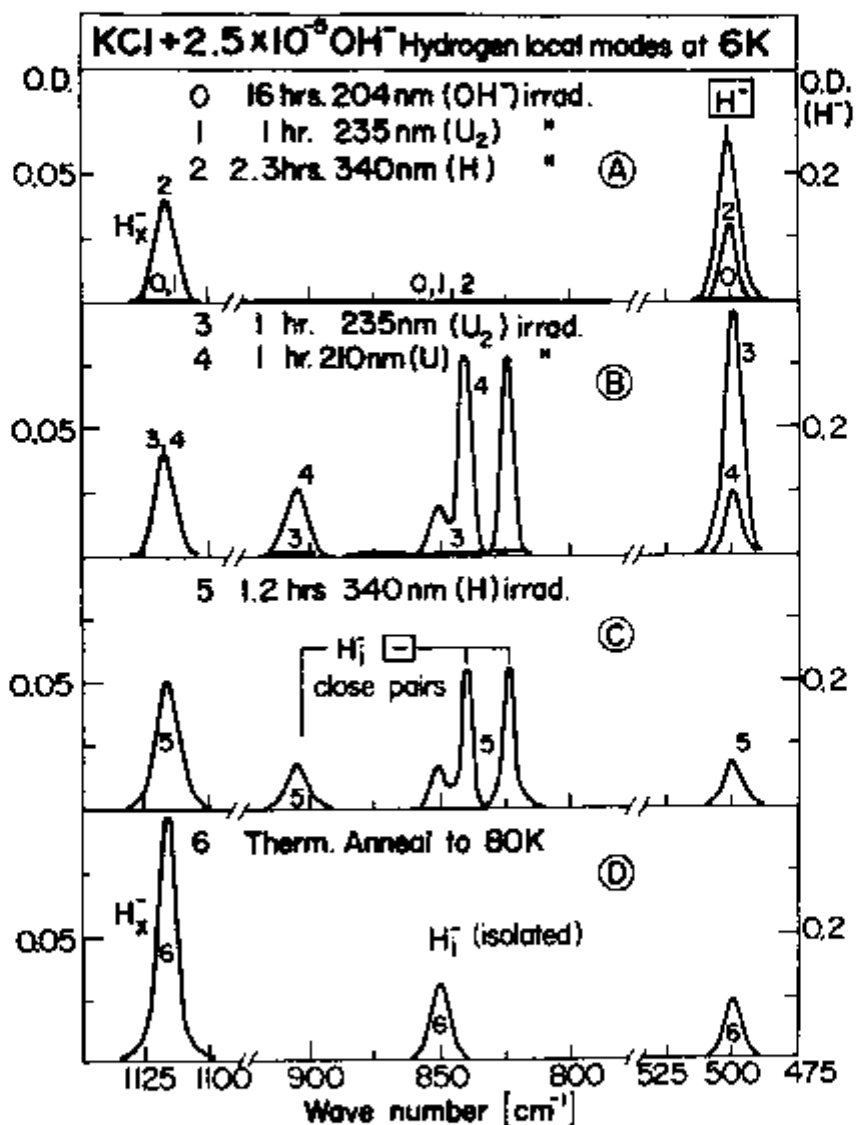

Figure 21 — Local mode transitions of H⁻, H_i^- and H_x^- under six different subsequent monochromatic irradiations at 6K (steps 0→5), and a final thermal annealing to 80K (step 6).

2 — **Production by thermal destruction of Cl_i^o crowdions.** The second possiblity to mobilize the Cl_i^o crowdions after their optical creation at LHeT is a thermal annealing process into the temperature range of their thermal instability ($T > 55°$). This process was performed as Step 6 in Figure 21D. It leads to a further considerable increase of the H_x^- centers and a simultaneous destruction of the $H_i^- /\boxed{-}$ close pairs. As the latter are clearly thermally stable in the used temperature range (they are thermally annealed only at $T > 90K^{(18)}$), we conclude that the H^- increase was achieved at the expense of the $H_i^- /\boxed{-}$ close pairs. (The H^- centers remained approximately constant during the thermal annealing Step 6.) Thus again we can conclude that thermally mobilized Cl_i^o crowdions form H_x^- centers by reacting with $H_i^- /\boxed{-}$ close pairs.

The involvent of the Cl_i^o in the H_x^- formation is conclusively demonstrated in Figure 22, in which we monitor the absorption of the Cl_i^o crowdions (H band) and the H_x^- local mode absorption during the thermal annealing process. The correspondence of the thermal destruction of the Cl_i^o centers (around 55K) to the increase of the H_x^- absorption is clearly demonstrated (the change in the H-band absorption at 10K is caused by thermal reorientation of the Cl_i^o crowdions).
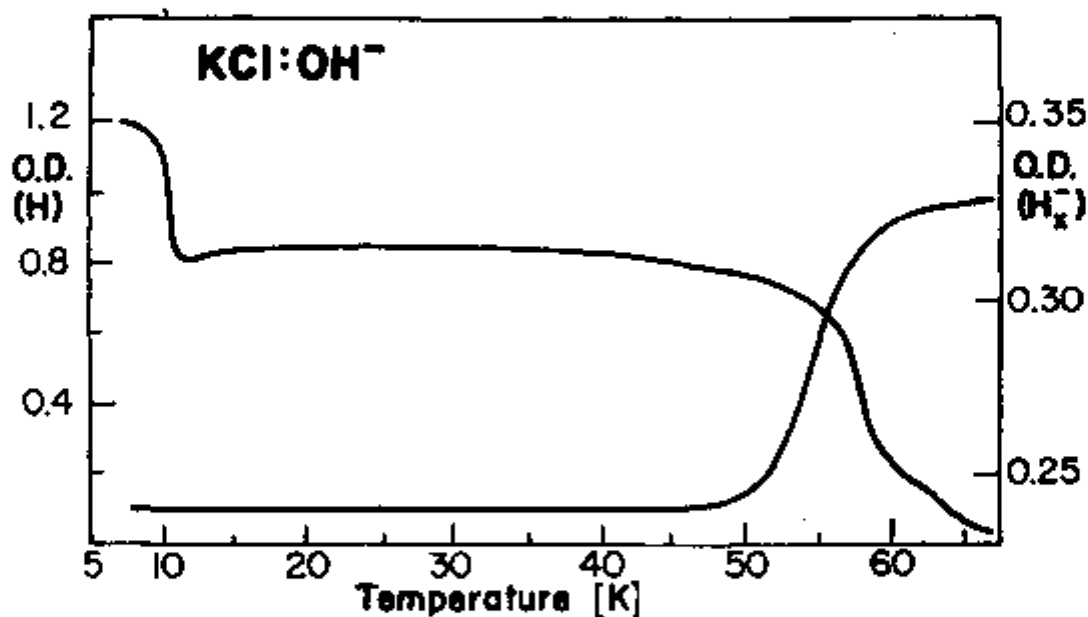

Figure 22 — H center decay and H_x^- buildup curves vs. temperature. This measurement corresponds to the experiment shown in Figure 21D.

3 — **Production by undispersed optical irradiation.** The two above results (items 1 and 2) were confirmed by a more general experiment where we employed undispersed broad band UV irradiation at 6K as we previously did at 77K. The results of this experiment are displayed in Figures 23A and 23B. From Figure 23A, Step 1, we see that after an exposure of undispersed UV light we observe immediate formation of all three hydrogen defects H_x^-, H_i^- (correlated and uncorrelated) and H^- centers. Since our irradiation contains the wavelengths of the OH^- band, of the different hydrogen centers involved (H^-, H_i^-, H_i^o), and of the H band absorption of the Cl_i^o center, the simultaneous appearances of the H_x^-, H_i^- and H^- centers is expected as in the LNT full irradiation case.

After this full UV exposure we bleached the H band using undispersed light but blocking any far UV light beyond 300 nm by a cut-off filter (see Step 2, Figure 23A). As previously observed, we again see the raise of the H_x^- at the expense of H_i centers. The following step was to practically repeat the previous UV treatment to re-establish the dynamical equilibrium among the three defects (Step 3, Figure 23A) as previously done at LNT.

As a last step, we performed again the thermal annealing to 77K procedure to make the crowdions thermally unstable. After this treatment we again observed an increase of H_x^- centers, a decrease of H_i^- centers (both correlated and uncorrelated) and a corresponding decrease of H^- centers. This experiment, although being different in terms of irradiation procedures and intermediate products obtained confirms the results of the previous monochromatic experiments.
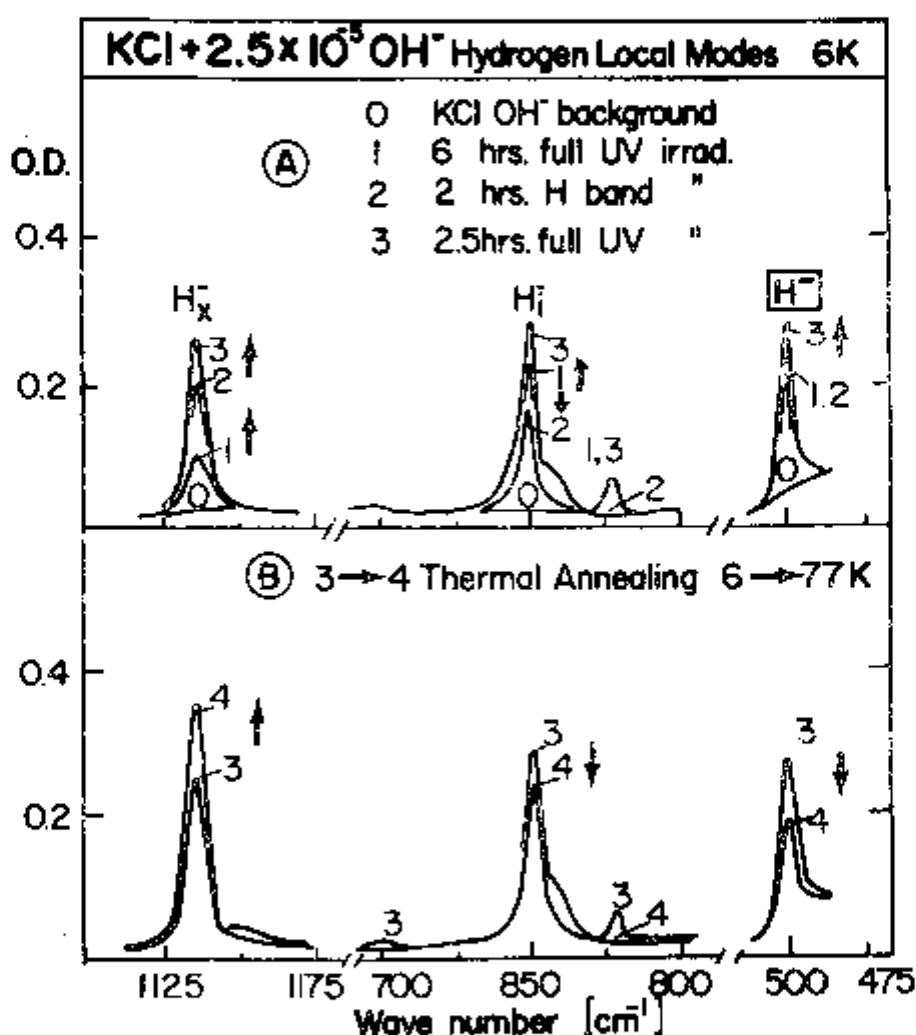
Figure 23 — Production of hydrogen centers in KCl:OH⁻ at 6K under undispersed light (broad band interference filter + Xenon lamp)
A — Step 1. Formation of H^-, H_i^- (different correlations) and H_x^- centers under full UV irradiation. Step 2. H_x^- formation and H_i^- destruction under H band (Cl⁰ crowdion) light. Step 3. Repetition of Step 1.
B — H_x^- production after a thermal annealing process to 77K. H_i^- and H^- centers decrease after this treatment.

F. THE THERMAL DESTRUCTION OF THE H_x^- CENTER.

To estimate the relative oscillator strength of the H_x^- center, we went back to Figure 11 where we see that at LNT approximately 50% less H^- centers are formed when compared to the LHeT experiment. We assume that the other 50% of "missing" H^- centers are being consumed to form H_x^- centers. Using the relative strengths of the integrated absorptions in Figure 13B, we obtain

$$f_{H_x^-} \, / \, f_H \; = \; 0.7$$

Considering the value 0.5 for the oscillator strength of the H^- center[18], we get approximately 0.35 for the oscillator strength of the H_x^- center.

After we have studied the detailed kinetics of the H_x^- center creation and concluded that the H_x^- center was the final and optically stable product of the OH^- photo-dissociation, we annealed a photodecomposed sample to investigate the thermal stability of the H_x^- center and the possible reaction products of the H_x^- thermal destruction.

When heating a sample containing H_x^- centers and following their local mode absorption at LNT after pulse annealing to various higher temperatures we found that the H_x^- centers decay thermally in the temperature range 180-210K (Figure 24B). This annealing behavior is very close to the $H_i^- \rightarrow \boxed{H^-}$ thermal decay process of H_i^- interstitials described by Fritz[18]. We indeed observed, together with the extinction of the H_x^- centers, this thermal reaction $H_i^- + \boxed{-} \rightarrow \boxed{H^-}$ by the H_i^- decrease and H^- increase, as shown in Figure 24A. A simple comparative analysis of the strengths of absorptions changes in the three IR bands involved in this process shows that the extinction of H_x^- centers does not create H^- centers.

Taking the loss in absorption strength in the H_x^- local mode ($\Delta OD \approx 0.8$) and converting it into the corresponding gain in absorption strength for the H^- center, we would expect an optical density increase of ~ 1.7 for the H^- absorption. We instead observed a mere 0.3 increase in O.D. of the H^- local mode, a fact that by itself excludes the possibility that the destruction of H_x^- centers will form H^- centers. The small increase of the H^- local mode is fully accounted for by the thermal destruction of the $H_i^- / -$ extrinsic Frenkel pairs, as seen by the destruction of the H_i^- local mode band. No new local mode absorption in the IR range and no new electronic absorption in the UV/Vis range is observed to develop after the thermal destruction of the H_x^- defects.

G. FINAL CONCLUSIONS ON THE H_x^- FORMATION PROCESS AND STRUCTURAL MODEL.

The large variety of experiments described in the previous sections offered a consistent picture about the two components which participate in the dynamic H_x^- center formation process.

a) Participation of a Cl_i^0 crowdion in the H_x^- center formation.

We proved in different ways that Cl_i^0 crowdions are participating in the H_x^- center formation:

(i) In the LNT range, where U_2 band irradiation creates the H_x^- defects, we showed that competing Na^+ defects can capture and stabilize Cl_i^0 crowdions and suppress the H_x^- formation.

(ii) Creating Cl_i^0 crowdions by X-rays at LNT in a KCl:H^- system leads to the formation of H_x^- (excluding the contribution of oxygen in any form in this process).

(iii) At LHeT we were able to create H_x^- centers stepwise in a controlled way by first creating stable Cl_i^0 crowdions. Only when these crowdions were made mobile by optical or thermal excitation, the H_x^- defects appear.

b) Participation of hydrogen defects in the H_x^- formation process.

The experiments under various temperature, irradiation, and defect conditions showed consistently:

(i) In a crystal containing both H_i^- /□ pairs and H^- defects, the formation of H_x^- centers is accompanied mostly by a reduction in close H_i^- /□ pairs and very little, if any, by a H^- defect reduction.

(ii) If only H^- defects are present, the H_x^- formation proceeds at the expense of the H^- defects.

From (a) and (b) above, we must conclude that the H_x^- defect is formed by the reaction of mobile Cl_i^0 crowdions with either close H_i^- /□ pairs (preferred process), or with H^- defects. As the H_i^- /□ Frenkel pair is — in terms of its net structural components — equivalent to the substitutional H^- defect, both these hydrogen traps for the Cl_i^0 crowdion can lead to the same end product.

From the H_x^- local mode strength, spectral shape and isotope shift we concluded that the defect must consist of a charged localized hydrogen defect in a site of high symmetry which does not split the local mode. The high frequency of the H_x^- local mode indicates a stronger vibrational potential of the H_x^- compared to the H_i^- defect.

From the thermal destruction of the H_x^- center we know that it is not converted back into H^- centers, but disappears into some unknown optically inaccessible structure.

A structural model must be able to integrate and satisfy all these static and dynamic experimental features. We see only one possiblity to achieve this in a single model: A hydrogen ion H^- in a body-centered interstitial position, with a trapped hole shared symmetrically by the four surrounding nearest neighbor anions (see Figure 25).

This model satisfies the observed static features, a localized charged hydrogen defect in a site high symmetry with a single unsplit three-fold degenerate local mode transition. Aside from the trapped hole, it is similar to the H_i defect (see Figure 25). In the latter one, the charged interstitial H_i defect will have strong electrostatic interactions with the surrounding ions, repelling and shifting outwards the anions, and attracting and pulling inwards the cations. The addition of a hole (positive charge) to the shell of nearest neighbor anions in the H_x^- center will reduce the $H_i^- \leftrightarrow Cl^-$ repulsion and thus produce a closer distance between the hydrogen and the chlorine ions. As the potential for the localized vibration of the H^- is mainly produced by the Born-Mayer repulsion interaction with the (large size) anions, we will expect a higher local mode frequency of the H_x^- compared to the H_i^- defect. This is in agreement with the frequency shift to higher energies found experimentally.

For the dynamic formation process, we have to regard the two cases:

a) Reaction of a Cl_i^0 crowdion with a close H_i^- /□ pair.

If the Cl_i^0 crowdion (an interstitial Cl_i^- ion with a bound hole) approaches a H_i^- /□ Frenkel pair, the most natural process to assume is the recombination of the Cl^- interstitial with the empty vacancy of the Frenkel pair. As a result we are left with the H_i^- interstitial and the hole which was
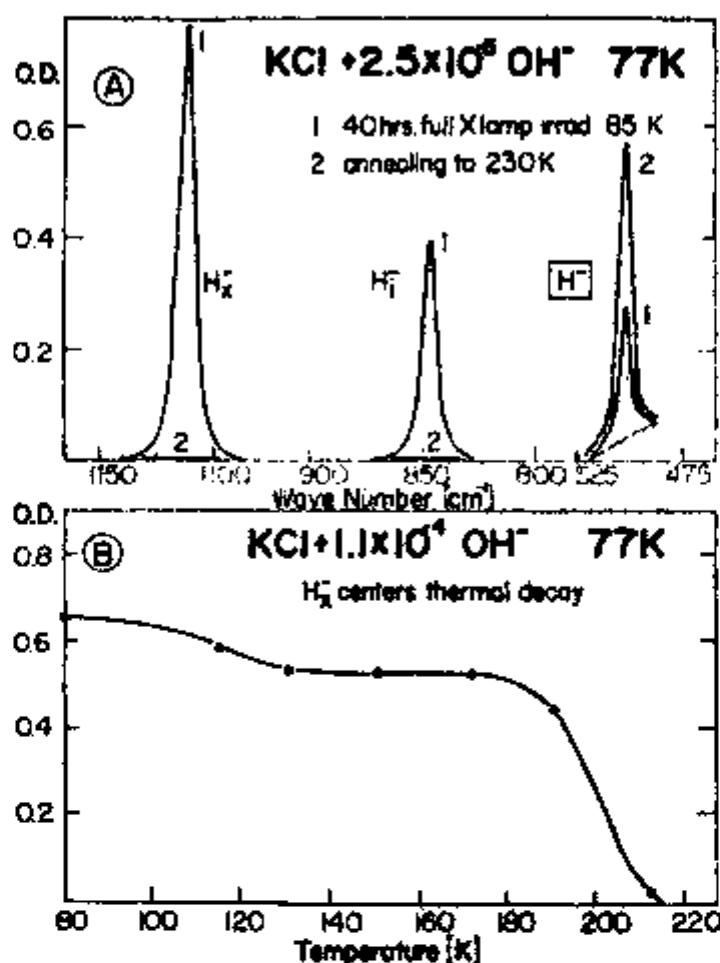
Figure 24 A — H_x^-, H_i^- and H^- centers local mode transitions before and after pulse annealing to 240K.
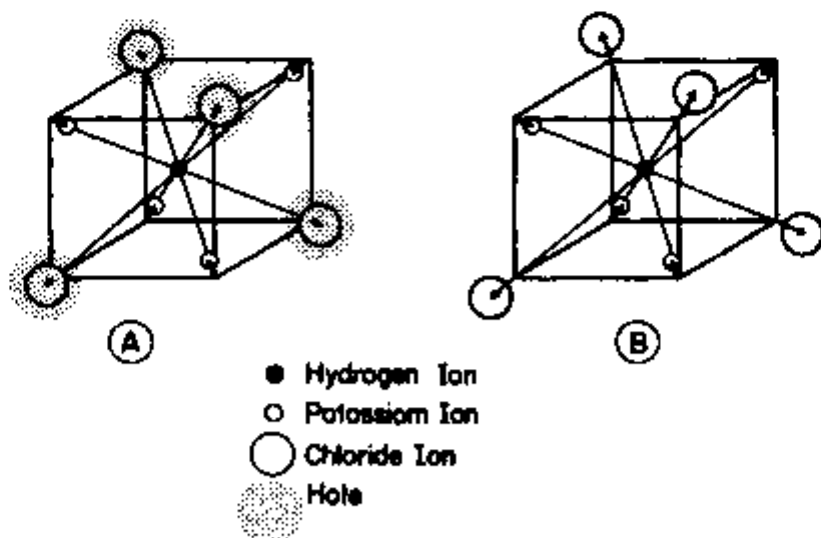B — H_x^- center annealing curve at LNT taken under a pulse annealing procedure.

Figure 25 — Structural model of the H_x^- center (A) and the H_i^- center (B) with indication of the shifts in position of the surrounding anions and cations due to electrostatic interaction with the interstitial hydrogen ion.

carried previously by the Cl_i^o crowdion. If this hole would just recombine with the interstitial H_i^- we would restore the original neutral interstitial H_i^o center. Apparently, however, the polarization of the surrounding ions around the H_i^- defect (Figure 25) make it possible to trap the hole at the Cl^- ions surrounding the H_i^- defect in a stable way.

b) Reaction of a Cl_i^o with a H^- defect.

In order to form the same H_x^- defect in this reaction, the approaching Cl^- interstitial crowdion will exchange the lattice place with the H^- defect, so that an interstitial H^- ion is formed. The hole, carried by the Cl_i^o crowdion then gets bound to the H_i^-defect in the same way as above.

In terms of its net components (after recombination of the hole with the H_i^- defect), the H_x^- defect is a neutral interstitial hydrogen atom. Thus when it gets thermally unstable and recombines with another H_x^- defect, it would form a neutral interstitial H_2 molecule. This defect is known to be present in alkali halides and spectrally invisible in both UV and IR range. The "spectral disappearance" of the H_x^- defect after thermal annealing is therefore well understandable with our model.

We should point out that the proposed model is constructed strictly from an extended static and dynamic experimental material, which — in our opinion — is conclusive and does not leave any alternative choice for a different model, consistent with the experiments. A theoretical justification for the proposed interstitial H^- structure with a stabilized hole shared by the surrounding anions is beyond the scope of this work. The theoretical understanding and justification for this peculiar "inverted and self-trapped exciton" at an interstitial hydrogen defect appears to be a challenging and interesting problem for further theoretical studies.

V — PHOTOREACTIONS OF KCl:OH⁻ BETWEEN 120 AND 200K.

RESULTS AND DISCUSSION

A. KCl:OH⁻ CRYSTALS.

In the previous chapter, we studied the OH^- photochemical reactions below 100K, where the most important product of the OH^- photodecomposition — the H_i^o center — was thermally stable. After this investigation was completed, the next question to be asked is: What happens to photodecomposed OH^- systems when one anneals it above the thermal stability of the H_i^o center?

1 — Thermal annealings above 120K. To answer the above question, we first photo-dissociated a KCl:OH⁻ crystal at LNT as usually done in the experiments of Chapter IV (see Figure 26). We then pulse annealed the system to 150K. During the heating cycle we followed the UV absorption vs. temperature of the H_i^o center and obtained its extinction curve which is displayed in the insert of Figure 26. After cooling back to LNT, we observed the formation of a broad band appearing in the F center region of the spectra. This band is assigned to the H_2O^- defect already reported by Rusch and Seidel[68].

The H_2O^- defect consists basically on a water molecule trapped by an F center with the unpaired F electron repelled from the water molecule, but still bound to the vacancy. The structure and properties of this center were extensively studied by Rusch[69] with EPR and ENDOR techniques. The optical absorption band of the H_2O^- center at LHeT shows a partly resolved structure with at least four bands in the vicinity of the F band. A proposed equation for the H_2O^- center formation is:

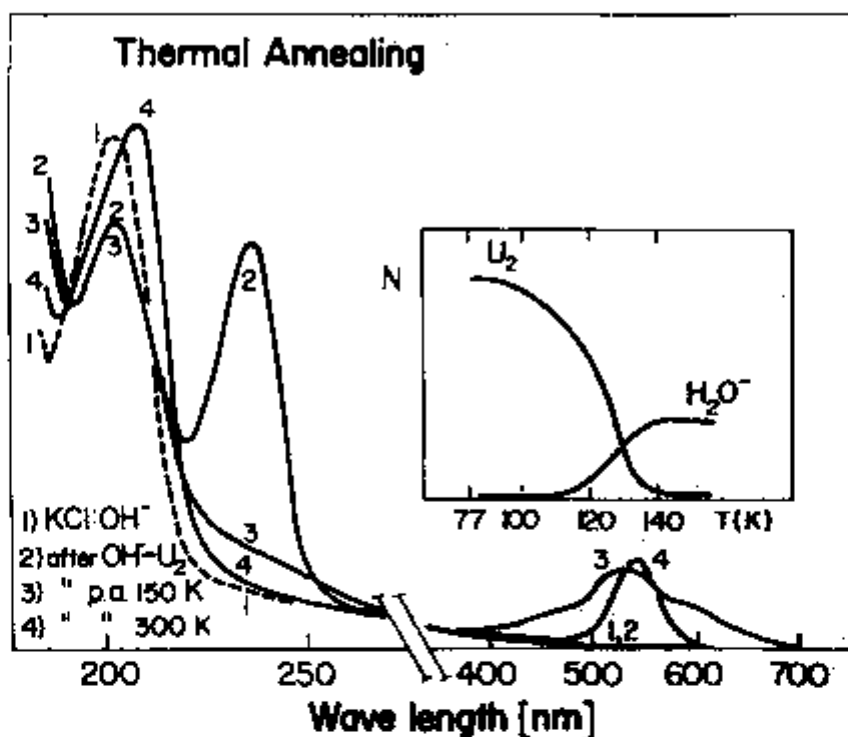$$\boxed{OH^-} + H_i^o + kT \rightarrow \boxed{H_2O^-} \qquad (22)$$

Figure 26 — Thermal annealing processes to 150 and 300K of a previously photodecomposed KCl:OH⁻ system at LNT. Insert: U_2 absorption band decrease and H_2O^- absorption band increase vs. temperature during the pulse annealing to 150K.

In another parallel experiment we followed the rise of the H_2O^- band and obtained its growth in optical density vs. temperature. This growth curve is displayed in the insert of Figure 26. A closer look at the H_i^o center extinction compared to the H_2O^- growth shows that the maximum rate of destruction of the H_i^o center coincides with the maximum rate of creation of the H_2O^- center. This aspect qualitatively confirms Equation (22) with respect to the origins of the H_2O^- center. However, we could not quantitatively follow the OH⁻ band behavior during this annealing process due to the formation of a strong background in the U_1 center region (Figure 26). It should be noted that the H_2O^- defect could as well have been formed by the reaction of the two thermally mobile interstitial H atoms (H_i^o centers) with the O^- defect (which should be available from the primary OH⁻ photodecomposition in large quantities) according to the following equation:

$$2 H_i^o + \boxed{O^-} + kT \rightarrow \boxed{H_2O^-} \tag{23}$$

To continue with our annealing procedures (H_2O^- centers are no longer stable above 200K), we made another pulse annealing to 300K which is also shown in Figure 26. In the visible we range observed the complete extinction of the H_2O^- center and the formation of a small quantity of F centers. As we can see from the relative oscillator strengths (see Table 2), the formed amount of F centers do not account for the number of H_2O^- destroyed. We should expect a factor of sixteen more F centers if we would assume that the water molecule goes to an interstitial position leaving the F center behind as proposed by Rusch and Seidel[68]. We will not try here to speculate on the fate of the H_2O^- center since another not understood center — the O^- — may be still available and could participate as well in high temperature reactions. We indeed observed a reduction of the U_1 center background in parallel with a decrease of the low energy tail at the O^- band. At the same time, a mixed OH⁻ and U center band appears which makes things more difficult for a quantitative analysis of the reaction products.

Since at high temperatures several centers become unstable, it is very difficult to control the various reactions that are simultaneously taking place. Reactions involving O^- and H^- ions are highly probable and stable molecules as O_2 or H_2 are likely to be formed in substitutional or interstitial positions and they would not be detectable by optical means. Due to these reasons we did not treat quantitatively the high temperature annealing results.

2 — Photodecomposition of OH^- centers at 150K. We next investigated the OH^- photodecomposition at temperatures above the thermal stability of the H_i° center. By irradiating into the OH^- band at 150K, we obtained its decrease accompanied by the increase of the H_2O^- band. This process is displayed in Figure 27. Plotting in a manner similar to the low temperature case, the OH^- and H_2O^- band changes vs. irradiation time (Figure 28A), and comparing the increase of the H_2O^- band with the OH^- band decrease (Figure 28B), we find the following results:

a) Compared to the LNT or LHeT OH^- photodecomposition, we observed that the initial quantum efficiency of OH^- destruction at 150K is a factor of two higher than it was at LNT or LHeT.

b) By plotting the OH^- absorption band decrease vs. H_2O^- absorption band increase, a linear relation between the OH^- decrease and H_2O^- increase is obtained (Figure 28B), indicating a direct conversion process between both centers without other side reactions.

The factor of two obtained between the OH^- destruction rates at LNT or LHeT and 150K indicates that for each H_2O^- center formed two OH^- centers were consumed — one by photodestruction process, and the other by trapping a mobile H_i° center. These observations suggested the following set of equations:

$$\boxed{OH^-} + h\nu \rightarrow \boxed{O^-} + H_i^\circ \tag{24}$$

$$2\boxed{OH^-} + h\nu + kT \rightarrow \boxed{O^-} + \boxed{H_2O^-} \tag{25}$$
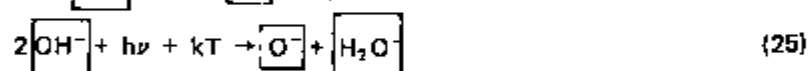
Adding these two equations, we obtain:

$$2\boxed{OH^-} + h\nu + kT \rightarrow \boxed{O^-} + \boxed{H_2O^-} \tag{26}$$
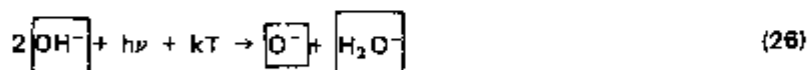
The slope taken from the straight line that correlates OH^- decrease with H_2O^- increase (Figure 28B) defines the relative oscillator strengths of these two bands (see Table 2). Unlike the low temperature case, the presence of F centers will now drastically alter the above discussed reactions. This will be treated in the next section.

B. KCl:OH⁻ CRYSTALS WITH F CENTERS.

1 — Thermal annealings above 120K. In the low temperature photodecomposition process of OH^- centers in a KCl:OH⁻ + F crystals we observed an initial decrease of F centers as reported in Section B of the previous chapter. The primary reactions in the presence of F centers were described by reaction-equations 14, 15 and 16, which postulate the production of H_i^- centers. As the electronic absorption (U_1 band) of these centers is hard to detect experimentally, we set up an experiment to directly observe the formation of the H_i^- center local mode in this process. The spectral changes in the UV and visible range during the initial OH^- photodecomposition are shown in Figure 29. In the insert of Figure 29, we display the rise of the H_i^- center local mode transition. This confirms further the validity of the equations 14, 15 and 16 describing the primary photoreactions appearing in the same experiment. Adding these equations we obtain for the net reaction:

$$\boxed{OH^-} + \boxed{e^-} + h\nu \rightarrow \boxed{O^-} + \boxed{} + H_i^- \tag{27}$$
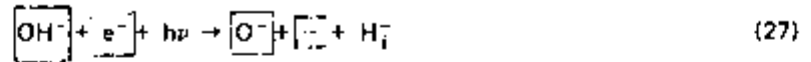
If we pulse anneal this photodecomposed system to 150K (Step 3 in Figure 29) we observe a strong increase of the H_i^- local mode band and a decrease in the F band (besides the thermal destruction of the U_2 band). The thermal annealing process makes the H_i^o mobile and possibly when it gets conveniently close to the F center, the F center ground state electron will tunnel to the H_i^o center which is thermally stable. It is interesting to note that in these reactions — and in the ones discussed for the KCl:OH$^-$ + F system previously in part IV, section B — interstitial hydrogen atoms never react with F centers to form an H$^-$ defect, a process which would appear to be very natural. Apparently, whenever a mobile H_i^o defect approaches an F center, a transfer of the F ground state electron to the interstitial hydrogen takes place at a certain distance (possibly by tunneling), forming and stabilizing the H_i^- defect. We never observed the reaction:

$$\boxed{e^-} + H_i^o \text{ (mobile)} \rightarrow \boxed{H_i^-} \tag{28}$$

but always instead the electron transfer reaction:

$$\boxed{e^-} + H_i^o \text{ (mobile)} \rightarrow \boxed{} + H_i^- \tag{29}$$

As a final procedure we pulse annealed our system from 150K to RT (Step 4 Figure 29). Above 200K, H_i^- centers are no longer stable. They will become mobile and eventually be trapped by their anti-center — the anion vacancy — and form the H$^-$ center. This process can clearly be observed in Figure 29. We then obtain the reaction:

$$H_i^- + \boxed{} + kT \rightarrow \boxed{H^-} \tag{30}$$

After this last process was completed we observed that the amount of F center reduction corresponds to the amount of U centers created. This fact confirms the above proposed equations to describe our observations. Adding all the equations that combine the OH$^-$ initial photodecomposition with the final thermal processes up to RT we end up with the net reaction:

$$\boxed{OH^-} + \boxed{e^-} + h\nu + kT \rightarrow \boxed{O^-} + \boxed{H^-} \tag{31}$$
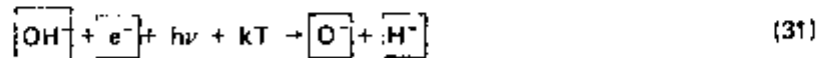
2 — Photodecomposition of OH$^-$ centers at 150K in the presence of F centers. Our next step was basically to repeat with KCl:OH$^-$ + F systems the experiments described in Section A-2 of this chapter. Now, in the presence of F centers the OH$^-$ photodecomposition process produces directly and very efficiently the destruction of F centers (see Figure 30) and the formation of H$^-$ and H_i^- centers. The presence of F light added to the UV irradiation basically does not influence the F decay process as can be seen in the insert of Figure 30. This fact led us to conclude that the tunneling process of the electron to a passing by H_i^o center is the most predominant process rather than an F center photo-ionization process. We should consider here that the formation of the H_2O^- center is taking place simultaneously, but due to the relatively small oscillator strength of the H_2O^- band, only very small changes in shape of the F band tails were observed.
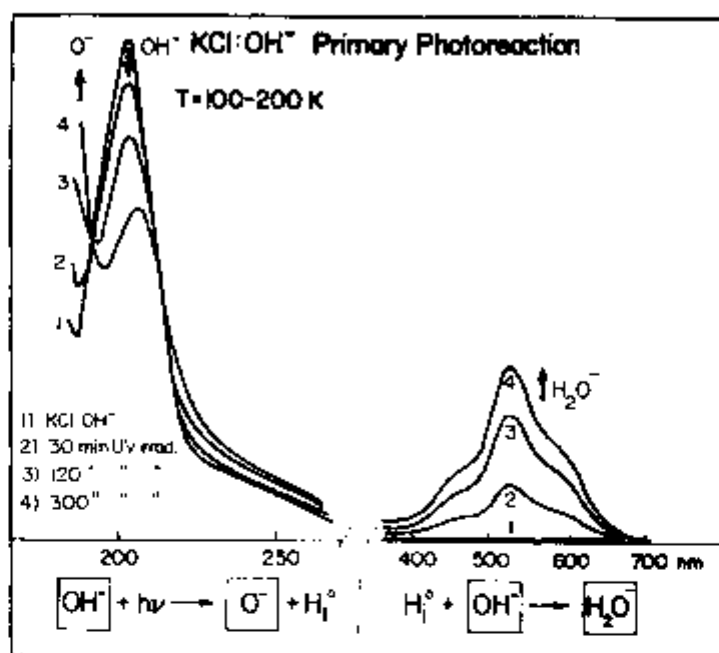
Figure 27 — Optical absorption spectra of a KCl:OH⁻ crystal, measured at 77K, showing the direct secondary product formation of the H₂O⁻ light irradiation.
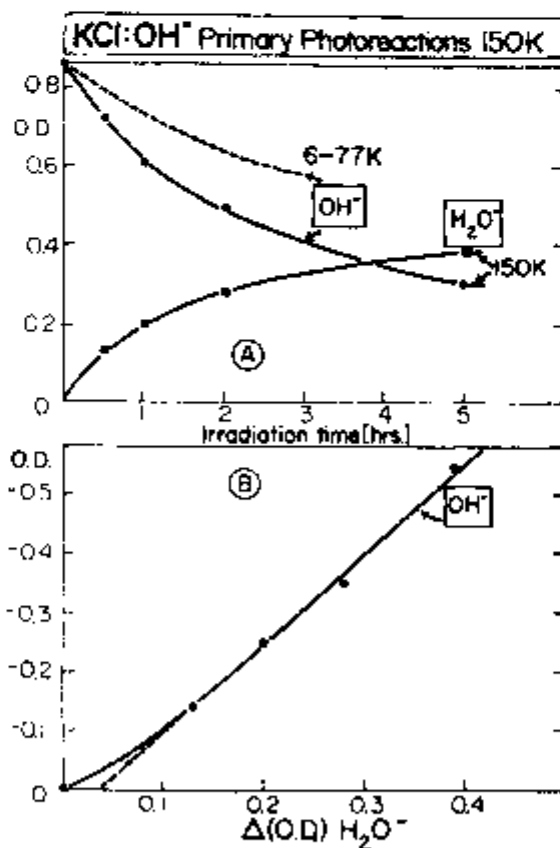

Figure 28 A — Direct secondary photo and thermal reaction rates at 150K. The dashed line indicates the OH⁻ band decay rate at 77K (measurements at 77K).

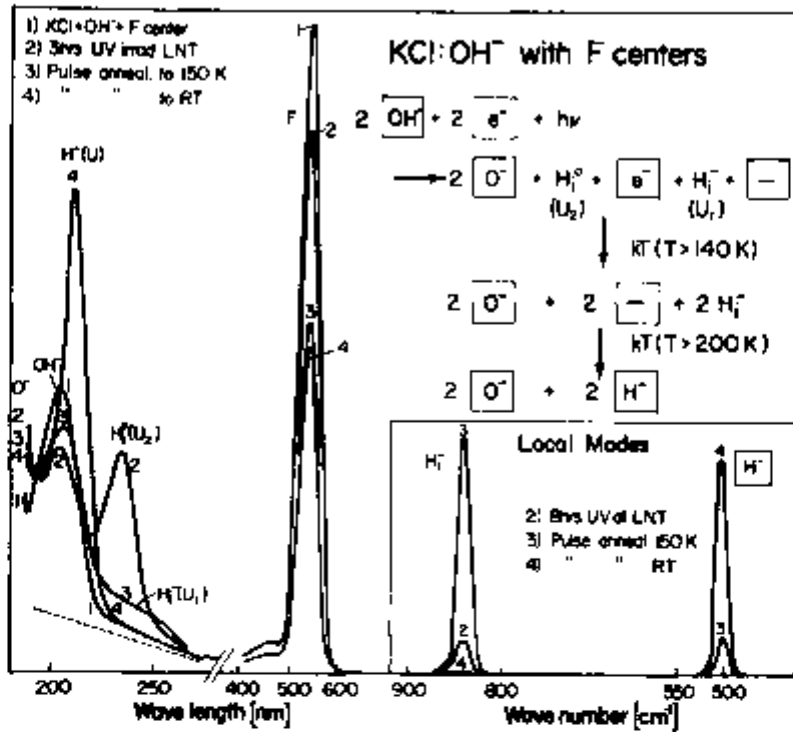B — Respective linear correlations observed between OH⁻ absorption band decrease and H₂O⁻ absorption band increase.

Figure 29 — Thermal annealing processes of a previous OH⁻ photo-dissociated KCl:OH⁻ + F system at 77K. Insert: Hydrogen center (H$_i^-$ and H⁻) local mode transitions.
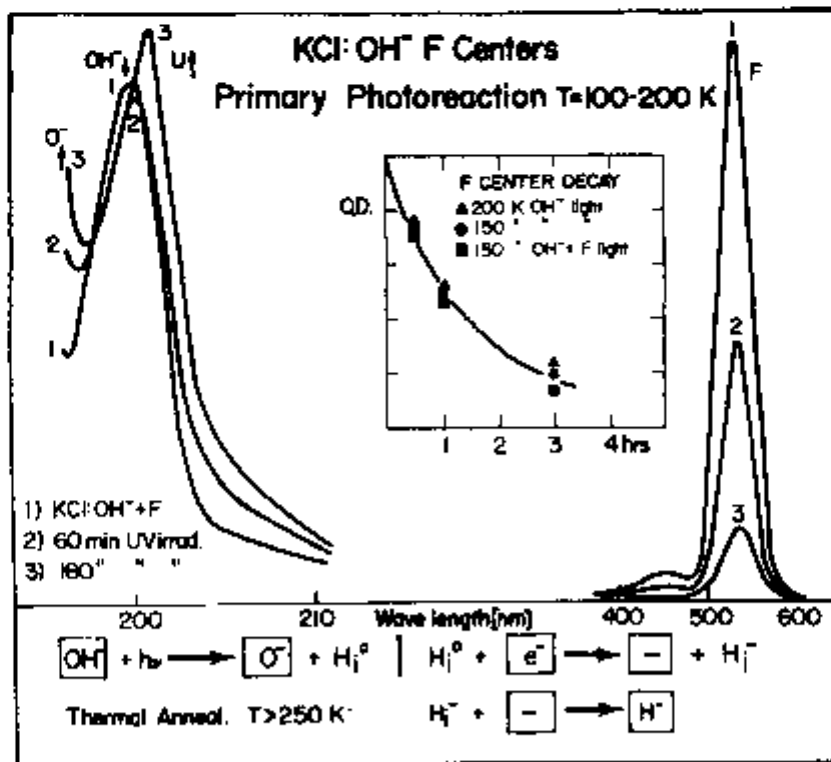

Figure 30 — Optical absorption spectra of a KCl:OH⁻ + F crystal measured at 77K after OH⁻ light irradiation at 150K Insert: F center decay curves for different temperature and irradiation conditions.

VI — PHOTOREACTION OF KCl:OH⁻ AROUND ROOM TEMPERATURE.

RESULTS AND DISCUSSION

A. KCl:OH⁻ CRYSTALS.

As previously mentioned, at higher temperatures (especially at RT) it is very hard — if not impossible — to control all the processes that are taking place simultaneously due to the instability and consequent mobility and aggregation of the different centers involved. Processes like interstitial molecules and colloid formations are usually the end products of high temperature photochemistry.

To get an idea of how a pure KCl:OH⁻ system would behave under OH⁻ light irradiation at RT, we basically repeated the experiments already done at lower temperatures. As one can see from Figure 31, very little change occured. We obtained a very small change (shift) in the original OH⁻ band in the UV region, possibly due to a very small amount of U-band development, and a small build-up of an F band. These results clearly show a high stability of the OH⁻ defect against optical bleaching at these high temperatures. As none of the primary and secondary reaction products treated at low temperatures (H_i^o, H_i^-, Cl_i^o, H_2O^-) remain stable (or stable trapping partners) at this high temperature, an efficient back-process apparently regenerates the OH⁻ center after its photo-dissociation.

B. KCl:OH⁻ CRYSTALS WITH F CENTERS.

In the presence of F centers the above situation changes somehow. At room temperature special care had to be taken to avoid any visible light while irradiating with monochromatic OH⁻ light since even small exposures to visible light would very efficiently aggregate F centers into F_2, F_3, etc. To achieve this desirable spectral purity of our UV light, we used two monochromators in tandem with a deuterium light source (low intensity visible light output) as described in Chapter III. The consequent loss in intensity was compensated by a prolonged UV exposure. The results of this experiment are presented in Figure 31B. We see in Steps 1 and 2 that the pure UV exposure is directly responsible for a partial conversion of F into U centers (no F center aggregation was observed at this stage). This is the same net process summarized by Equation (30).

The OH⁻ photo-dissociation of the KCl:OH⁻ + F system, thermally annealed to RT (e.g., curve 3 in Figure 29) produces a similar net result as direct photo-dissociation at RT. A subsequent short time F light exposure of the crystal (Step 3 in Figure 31B) produces immediatly F center aggregation, a totally independent and well known process that did not bring any change to the UV spectrum

The same original KCl:OH⁻ + F crystal, when exposed at RT to the full undispersed irradiation of a Xenon lamp, showed initially that the process described in Equation (32) was indeed taking place. After an appropriate irradiation time — 4.5 hours (Step 3 in Figure 32) — one obtains an almost complete destruction of all F centers and visible absorption in the crystal (shown in Step 3, Figure 32). Now if the undispersed irradiation is extended further for prolonged times, new photochemical processes take place: in the UV range the U-band is bleached and transformed into a new unidentified absorption band in higher energies, while in the visible range, the formation of the colloid band[70] is observed.

It was not our intent to study and try to understand these high temperature photoreactions in any detail. They were undertaken after the detailed and quantitative low temperature photochemistry study, to obtain a qualitative survey about the following high temperature photochemistry.

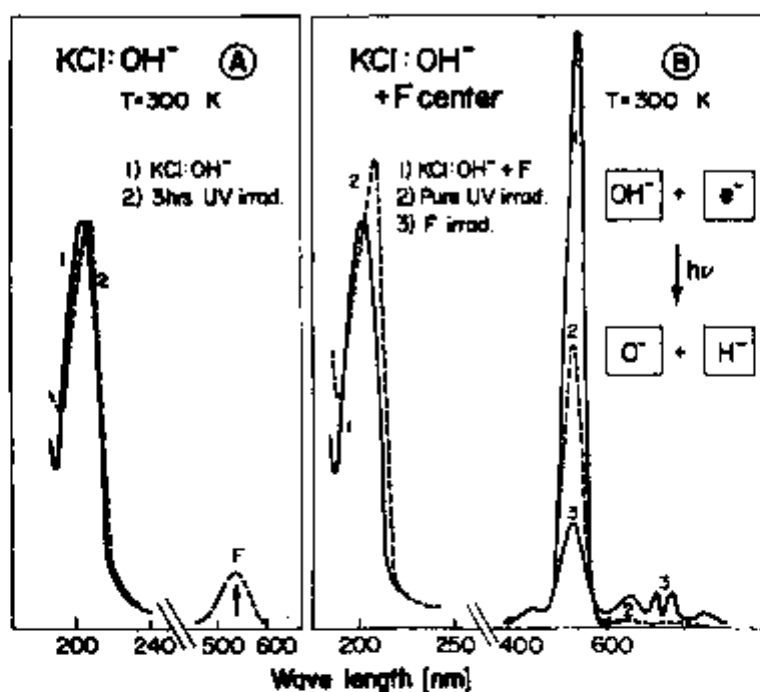The role of the F centers as extra reaction and trapping sites in the OH⁻ photochemistry can

Figure 31 A — UV irradiation of a KCl:OH⁻ system at room temperature.
B — 204 nm (tandem monochromators) UV irradiation of a KCl:OH⁻ + F system at room temperature (measured at 77K).
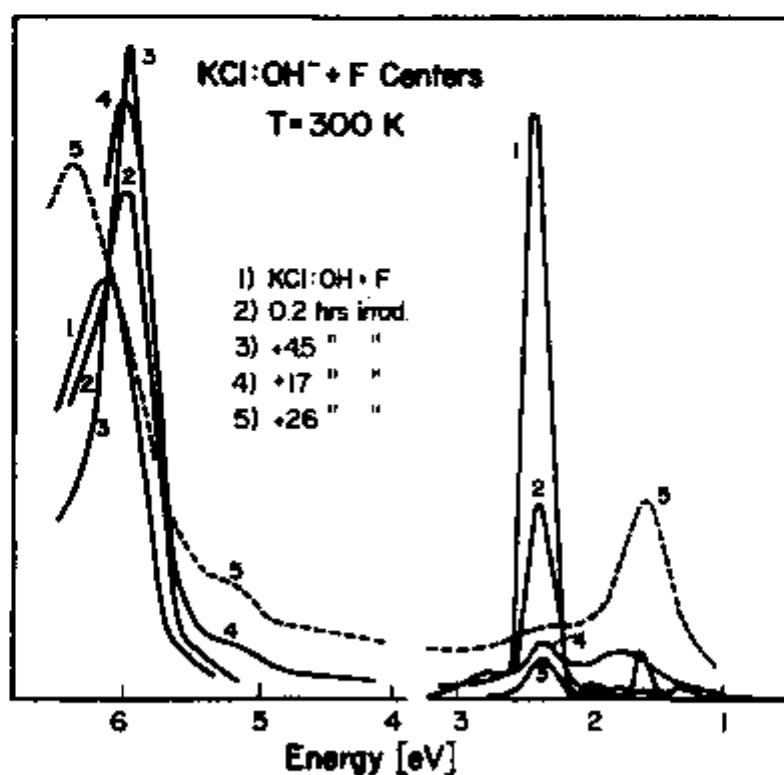

Figure 32 — KCl:OH⁻ + F system under full Xenon lamp irradiation at room temperature (. measured at 77K).

be summarized as follows: at low temperatures, where basically all primary and secondary reactions products of the OH^- dissociation are thermally stable, the extra F centers have little influence on these reactions. Towards higher temperatures, with increasing instability of the OH^- reaction products, the role of the F center as trapping- or reaction sites becomes more and more decisive. At RT, in fact, the OH^- photodecomposition (not present in the pure crystal), becomes possibly only by the presence of F centers.

The observation and understanding of the highly efficient F center bleaching effect by UV light in $KCl:OH^-$ crystals opens another line of possibilities: for potential application of color centers in optical information storage and to the production of U-aggregate centers. We will briefly discuss these possibilities in the next chapter.

VII – F CENTER BLEACHING BY UV LIGHT IN $KCl:OH^-$ CRYSTALS AND ITS POSSIBLE SIGNIFICANCE FOR INFORMATION STORE AND U_A CENTER PRODUCTION.

A. OPTICAL INFORMATION STORAGE.

Pure additively colored crystals are well known for their stability against a permanent bleaching of their coloration. Under visible light alone, these systems show the reversible $F \rightarrow F'$ reaction at low temperatures[71] and the aggregation into complexes F_2, F_3, etc., at high temperatures[72]. When irradiating with visible light into F center systems that also contain OH^- impurities, no new effects are observed. We again obtain the reversible $F \rightarrow F'$ conversion at low temperatures and the F center aggregation at high temperatures.

These properties, however, change drastically in $KCl:OH^-$ crystals if our irradiation contains UV light as we showed in this work. Under OH^- light irradiation, we were able to produce in a very broad temperature range an almost complete and irreversible destruction of F centers and any visible absorption in the crystal under UV light irradiation. This bleaching effect was partially reversible only after heating the samples to $650°C$ when we observed a return of part of the F centers.

In Figure 33 we summarize the decay of the F center vs. UV irradiation time for several temperatures of study. We see that this process has a small bleaching quantum efficiency at temperatures where $H_i^°$ centers are thermally stable. The maximum bleaching occurred at 150K. At room temperature, although we had an initially high efficiency, the process saturated relatively fast. These mixed $KCl:OH^- + F$ crystals therefore allow us to make a UV light irradiation process visible by the bleaching of color (absorption band) in the visible spectral range. It is evident that this ability makes this crystal system interesting as a photochromic material for the storage of optical information. This general field has received in the last decade a lot of attention: three-dimensional "Bragg-angle holograms" have, for instance, been stored in large numbers by optical alignment of F_A centers in $KCl:Na^+$ crystals[73].

To demonstrate qualitatively in the simplest way these photochromic properties of the $KCl:OH^- + F$ material under UV irradiation, we produced some images in these crystals by a sample shadow process.

The obtained contrast is remarkably high (60:1) and the images are stable at room temperature and normal light (containing no far UV components). In figure 34 we display several different patterns obtained with these crystals under different temperature conditions. The finest grid structure used had a density of 1200 "images" per cm^2. (The resolution of this grainless photochromic material is basically unlimited)

The reversibility of this process is only partial. Under annealing to high temperatures ($650°C$), only part of the original F centers are restored. This does not encourage the

52

use for repeated "write-read-erase..." application as required for computer memory. Nevertheless, this material appears excellent to optically register permanent planar or volumetric information carried by UV irradiation. With the present advent of UV lasers, holographic information storage in these systems may be a definite possibility.
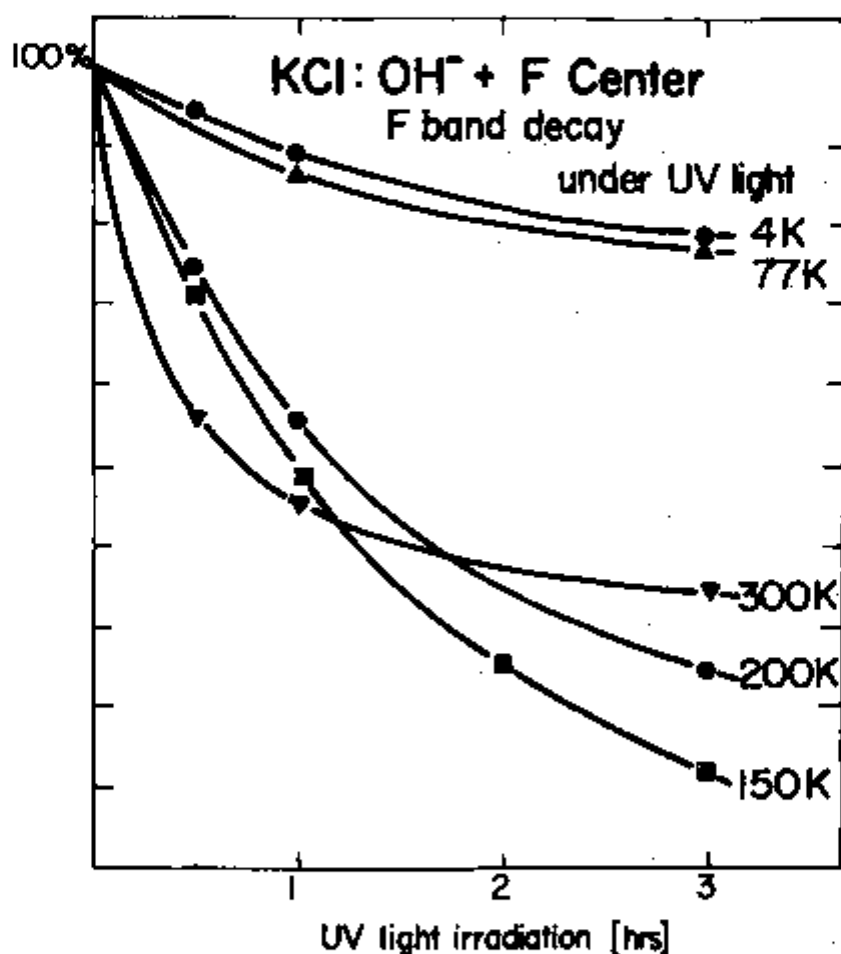

Figure 33 — F center decay curves in a KCl·OH⁻ + F crystal under OH⁻ light irradiation for different temperatures.
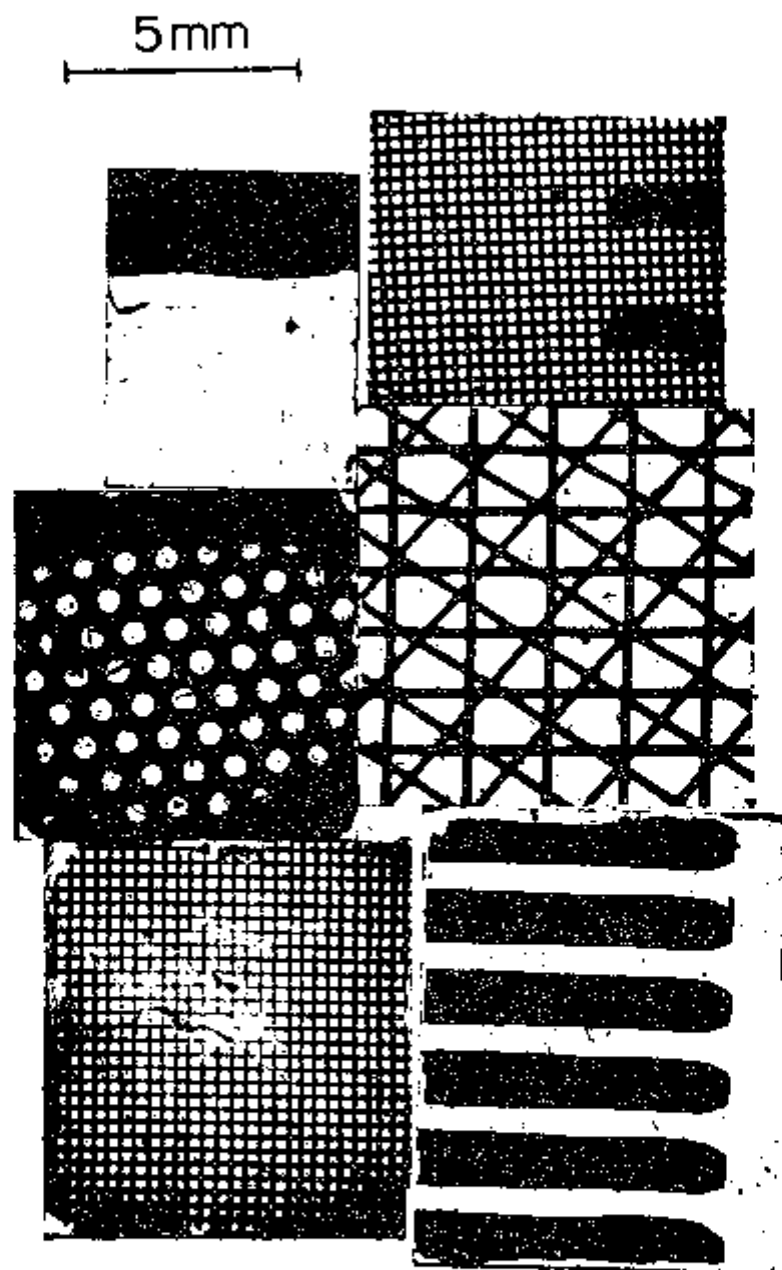
Figure 34 — Photograph of an array of six KCl:OH⁻ + F samples in which we produced different forms of high contrast visible imagens. Clockwise from the upper left: (1) High contrast (60:1) produced by full Xenon lamp irradiation and annealed to RT. (2) Same as (1). (3), (4), (5), and (6) were produced at RT under full Xenon lamp irradiation.

B. CONTROLLED PRODUCTION OF U_A CENTERS.

If our KCl system contains, besides the OH^- and F centers, metallic impurities such as the Na^+ , we are able to convert F centers almost entirely into F_A centers, according to the following equation:

$$e^- + \boxed{Na^+} \rightarrow \boxed{e^- \;|\; Na^+} \;(F_A) \tag{33}$$

Proceeding with the OH^- photodecomposition at 150K in such a crystal with F_A centers and then annealing to room temperature, we were able to end up with U_A centers (a substitutional hydrogen ion having a Na^+ impurity as one of the nearest neighbors). Their effective net process can be described by the following equation:

$$\boxed{e^-} + \boxed{Na^+} + \boxed{OH^-} + h\nu + kT \rightarrow \boxed{O^-} + \{\boxed{H^- \;|\; Na^+}\} \tag{34}$$
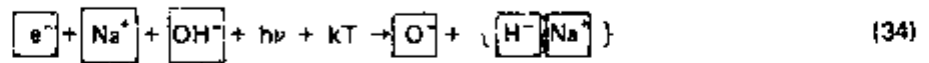
An indication for the presence of this process is displayed in Figure 35. The nearest neighbor metallic impurity reduces the O_h cubic symmetry into C_{4v} resulting in a splitting of the three-fold degenerate U center local mode transition into a singlet and a doublet[74]. In figure 35 is displayed the "γ_1 line" attributed to the E_g double degenerate mode. This first rough experiment demonstrates the possibility to create U_A centers in a controlled way (so far, U_A centers were observed only statistically in heavily doped crystals with metallic impurities and U centers). This method for creating U centers with locally reduced symmetry (even optically aligned ones!) appears to be very promising for further local mode studies.
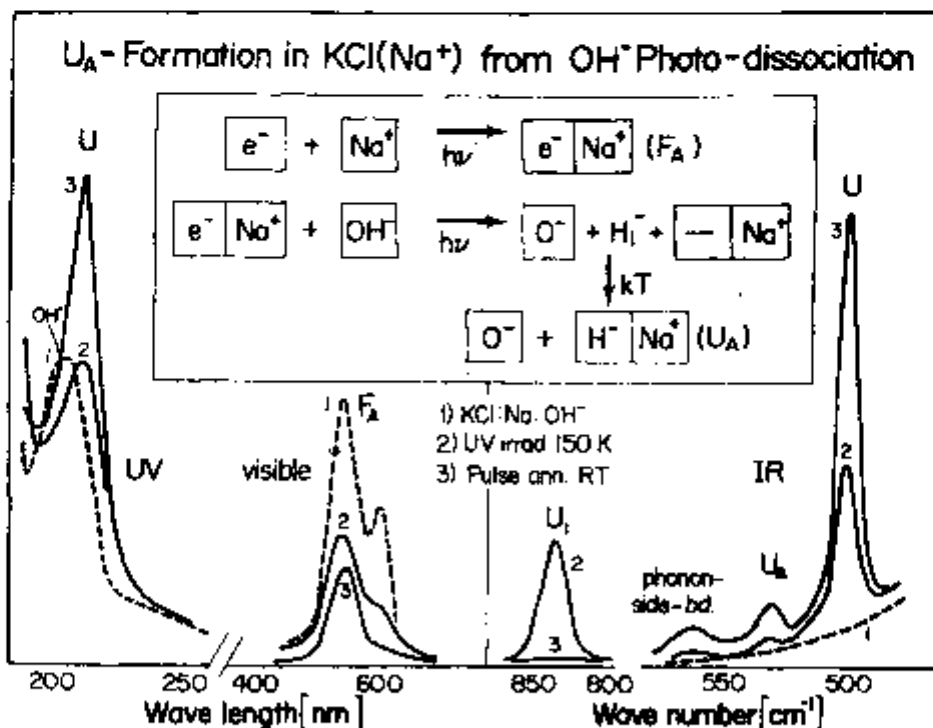

Figure 35 — U_A center formation in a KCl:OH^- + Na^+ + F system obtained after the following steps:
(a) F → F_A conversion at -15°C.
(b) OH^- photodecomposition at 150K.
(c) Anneal to room temperature (measurements at 77K).

BIBLIOGRAPHY *

1. J. Rolfe, Phys. Rev. Letters 1, 56 (1958).

2. H. W. Etzel and D. A. Patterson, Phys. Rev. 112, 1112 (1958).

3. W. Kanzig, H. R. Hart, and S. Roberts, Phys. Rev. Letters 13, 543 (1964).

4. Bosshard, R. W. Dreyfus and W. Kanzing, Phys. Kondensierte Materie 4, 254 (1965).

5. K. Brugger and W. P. Mason, Phys. Rev. Letters 7, 270 (1961).

6. K. Brugger, T. C. Fritz and D. A. Kleinman, J. Acoust. Soc. Am. 41, 1015 (1967).

7. B. Fritz, F. Lüty, and J. Anger, Z. Physik 174, 240 (1963).

8. M. V. Klein, Phys. Rev. 122, 1393 (1961).

9. F. Kerkoff, Z. Physik 158, 595 (1960).

10. J. A. Caps, Phys. Rev. 122, 18 (1968).

11. F. Lüty, J. Phys. Chem. Solids 23, 677 (1962).

12. U. Kuhn and F. Lüty, Solid State Comm. 2, 281 (1964).

13. A. S. Nowick and W. R. Heller, Adv. Phys. 12, 251 (1963).

14. S. Kapphan and F. Lüty, J. Phys. Chem. Solids 34, 969 (1973).

15. H. Hartel and F. Lüty, Phys. Stat. Sol. 12, 347 (1965).

16. C. J. Delbecq, B. Smaller and P. H. Yuster, Phys. Rev. 104, 599 (1956).

17. G. Schaefer, J. Phys. Chem. Solids 12, 233 (1960).

18. B. Fritz, J. Phys. Chem. Solids 23, 375 (1962).

19. For a recent review see D. Pooley and W. A. Sibley in "Color Centers and Radiation Damage" AERE Report R-7347 Harwell, January 1973.

20. G. Kurz, Phys. Stat. Sol. 31, 93 (1969).

21. M. R. Tubbs and D. K. Wright, Phys. Stat. Sol. (a) 7, 155 (1971).

22. H. Blume, T. Bader and F. Lüty, Optics Commun. 12, 147 (1974).

23. H. Paus and F. Lüty, Phys. Stat. Sol. 12, 341 (1965).

24. R. Hilsch and R. W. Pohl, Gottingen Nachrichten 322 (1933).

25. W. Martianssen, Phys. Chem. Solids $\underline{2}$, 257 (1957).

26. D. G. Chae and B. G. Dick, J. Phys. Chem. Solids $\underline{34}$, 1683 (1973).

27. C. K. Chau, M Klein and B. Wedding, Phys. Rev. Letters $\underline{17}$, 521 (1966).

28. D. A. Patterson and M. N. Kabler, Solid State Comm. $\underline{3}$, 75 (1965).

29. H Kostlin, Solid State Comm. $\underline{3}$, 81 (1965).

30. E. Sonder and W. A. Sibley, Point Defects in Solids Vol. 1, ed. J. H. Crawford, Jr. and C. M. Slifkin, Plenum Press, New York 1972 (p. 201).

31. H. Bauser and F. Lüty, Phys. Stat. Sol. $\underline{1}$, 608 (1961).

32 M. Hirai, Y. Kondo, T. Yoshinari and M. Ueta, J. Phys. Soc. Japan $\underline{30}$,440 (1971).

33. Y Kondo, M. Hirai and M. Ueta, J. Phys. Soc. Japan $\underline{33}$, 151 (1972).

34. Y Toyozawa, Proceedings of the 1974 International Conference on Color Centers in Ionic Crystals, Sendai, Japan, Communication #D43.

35. G Kurz and W Gebhardt, Phys. Stat. Sol. $\underline{7}$, 351 (1964).

36. C J Delbecq, J. L. Kolopus, E. C. Yasaitis and P. H. Yuster, Phys. Rev. $\underline{154}$, 866 (1967).

37. C. J Delbecq, D Hutchinson, D. Schoemaker, E. L. Yasitis and P. H. Yuster, Phys. Rev. $\underline{187}$, 1103 (1969).

38. N. Itoh and M. Ikeya, J. Phys. Soc. Japan $\underline{22}$, 1170 (1967).

39. R W. Pohl, Proc. Phys. Soc. $\underline{49}$, 3 (1937).

40. R Hilsch and R. W. Pohl, Trans. Faraday Soc. $\underline{34}$, 883 (1938).

41. A Hausmann, Zeits, F. Physik $\underline{192}$, 313 (1966).

42. J. M. Spaeth, Zeits. f Physik $\underline{192}$, 107 (1966).

43. W. Hayes and J W. Hodby, Proc. Roy. Soc. $\underline{A294}$, 359 (1966).

44. F Lüty, S. Costa Ribeiro, S. Mascarenhas and V. Sverzut, Phys. Rev. $\underline{168}$, 1080 (1968).

45. M. Hirai, J. Phys. Soc. Japan $\underline{15}$, 1308 (1960).

46. G. Kurz and S. Susman, Proceedings of the 1971 International Conference on Color Centers in Ionic Crystals, Reading, England, Communication #105.

47 M. de Souza and F. Lüty, Phys. Rev. $\underline{8}$, 5866 (1973).

48. G K. White, *Experimental Techniques in Low Temperature Physics*, 2nd ed., Oxford (1968).

49. N. F. Mott and R. W. Gurney, *Electronic Processes in Ionic Crystals*, 2nd ed., Dover, New York 1964.

50 F. Seitz, Modern Theory of Solids, McGraw Hill, New York 1940.

51. A. B. Scott, W. A. Smith and M. A. Thompson, J. Phys. Chem. 57, 757(1953).

52 C. Z. Van Doorn, Rev. Sci. Instr. 32, 755 (1961).

53 Von H. Rogener, Ann. der Physik 29, 386 (1937).

54 F. Rosenberger, Mat. Res. Bull. 1, 55 (1966).

55. F. J. Kopp and T. Ashworth, Rev. Sci. Instr. 43, 327 (1972).

56. A. Smakula, Zeits f. Physik 59, 603 (1930).

57. F. Kerkoff, W. Martienssen and W. Sander, Z. Physik 173, 184 (1963).

58. J. M. Spaeth, private communication.

59. W. Sander, Z. Physik 169, 353 (1962).

60. J. M. Spaeth and M. Storm, Phys. Stat. Sol. 42, 739 (1970).

61. J. M. Spaeth and H. Seidel, Phys. Stat. Sol. 46, 323 (1971).

62. G. Reuter, L. Schwan and J. M. Spaeth, Phys. Stat. Sol. (b) 53, K29 (1972).

63. M. H. Wagner and J. M. Spaeth, Solid State Comm. 14, 1101 (1974).

64. F Fischer and H. Gründing, Z. Physik 184,299 (1965).

65. J. Rolfe, Appl. Phys. Letters 6, 66 (1965).

66. W. D. Avering and J. J. Markham, Phys. Rev. 88, 1043 (1952).

67. B Fritz, J. Phys. Chem. Solids, Suppl. 1, 485 (1965).

68 W. Rush and H Seidel, Solid State Comm. 9, 231 (1971).

69. W. Rush, Dr. Thesis, Stuttgart 1972.

70. A. B. Scott and L. Bupp, Phys. Rev. 79, 341 (1950).

71. H. Fedders, M. Hunger and F. Lüty, J. Phys. Chem. Solids 22, 299 (1961).

72 F Seitz, Rev. Mod. Phys. 18, 384 (1946).

73. F. Lüty in "Physics of Color Centers". Cap.3, edited by W. B. Fowler, Academic Press (1968).

74. D. N. Mirlin and I. I. Reshina, Soviet Phys. Sol. State 8, 116 (1966).